Defense Threat Reduction Agency
8725 John J. Kingman Road, MS 6201
Fort Belvoir, VA 22060-6201

DTRA-TR-01-16

TECHNICAL REPORT

Application of Soviet PNE Data to the Improvement of Seismic Monitoring Capability

Approved for public release; distribution is unlimited.

August 2004

DSWA 01-97-C-0126

John R. Murphy , et al.

Prepared by:
Titan Pulse Sciences Division
2700 Merced St.
San Leandro, CA 94577-0599

DESTRUCTION NOTICE:

Destroy this report when it is no longer needed.
Do not return to sender.

PLEASE NOTIFY THE DEFENSE THREAT REDUCTION AGENCY, ATTN: BDMI, 8725 JOHN J. KINGMAN ROAD, MS-6201, FT BELVOIR, VA 22060-6201, IF YOUR ADDRESS IS INCORRECT, IF YOU WISH IT DELETED FROM THE DISTRIBUTION LIST, OR IF THE ADDRESSEE IS NO LONGER EMPLOYED BY YOUR ORGANIZATION.

REPORT DOCUMENTATION PAGE

Form Approved

1. AGENCY USE ONLY *(Leave blank)*	2. REPORT DATE	3. REPORT TYPE AND DATES COVERED
	040800	Technical 970922-001101

4. TITLE AND SUBTITLE

Application of Soviet PNE Data to the Improvement of Seismic Monitoring Capability

5. FUNDING NUMBERS

C – DSWA01-97-C-0126
PE – 463D
PR – CD
TA – CD
WU – DH003590

6. AUTHOR(S)

John R. Murphy, Brian W. Barker, and Margaret E. Marshall (T P S D)

Jamil D. Sultanov and Ivan O. Kitov (I D G)

7. PERFORMING ORGANIZATION NAME(S) AND ADDRESS(ES)

Titan Pulse Sciences Division
2700 Merced St.
San Leandro, CA 94577-0599

8. PERFORMING ORGANIZATION REPORT NUMBER

MSD-DFR-00-16613

9. SPONSORING/MONITORING AGENCY NAME(S) AND ADDRESS(ES)

Defense Threat Reduction Agency
8725 John J. Kingman Road, MSC-6201
Fort Belvoir, VA 22060-6201

TDND/Barber

10. SPONSORING/MONITORING AGENCY REPORT NUMBER

DTRA-TR-01-16

11. SUPPLEMENTARY NOTES

This work was sponsored by the Defense Threat Reduction Agency under RDT&E RMC Code B 463 D CD CD 25904D.

12a. DISTRIBUTION/AVAILABILITY STATEMENT

Approved for public release; distribution is unlimited.

12b. DISTRIBUTION CODE

13. ABSTRACT *(Maximum 200 words)*

This report provides a summary of the results of a joint research program which has been carried out by scientist from Maxwell Technologies, Inc. and the Russian Institute for Dynamics of the Geospheres to use regional seismic data recorded from Soviet PNE test and nearby earthquakes and mining events to assess the applicability of various proposed discriminants over the wide ranges of source and propagation path characteristics sampled by these test. This research has encompassed the formulation of a seismic source summary for 122 Soviet PNE test, a discrimination analysis of broadband seismic data recorded from a number of these PNE events and nearby earthquakes at the Borovoye Geophysical Observatory and a variety of temporary stations, a comparison of near-regional signals recorded by nearby tamped chemical and nuclear explosions at the Soviet Degelen Mountain test site and an analysis of the characteristics of the explosion aftershocks observed following selected Soviet PNE tests.

14. SUBJECT TERMS

Soviet PNE, Regional, Monitoring, Seismic, Explosion Aftershocks, Discrimination, Borovoye, Degelen, Source Summary

15. NUMBER OF PAGES

76

16. PRICE CODE

17. SECURITY CLASSIFICATION OF REPORT	18. SECURITY CLASSIFICATION OF THIS PAGE	19. SECURITY CLASSIFICATION OF ABSTRACT	20. LIMITATION OF ABSTRACT
UNCLASSIFIED	UNCLASSIFIED	UNCLASSIFIED	SAR

NSN 7540-01-280-5500

Standard Form 298 (Rev. 2-89)
Prescribed by ANSI Sta. 239-1298-102

CLASSIFIED BY:
N/A since Unclassified

DECLASSIFY ON:
N/A since Unclassified

7. PERFORMING ORANIZATION NAME(S) AND ADDRESS(ES) (Continued)

Institute for Dynamics of the Geospheres
The Russian Academy of Sciences
Leninsky Prospect, 38
Korpus 6
Moscow, Russia 117979

SUMMARY

This report has provided a summary of the results of a joint research program which has been carried out by scientists from Maxwell Technologies, Inc. and the Russian Institute for Dynamics of the Geospheres (IDG) in an attempt to derive improved, quantitative constraints on the transportability of various regional discriminants as they apply to the identification of underground nuclear explosions under the CTBT. In particular, regional seismic data recorded from Soviet PNE tests and nearby earthquakes and mining events have been collected and analyzed to further test the applicability of various proposed discriminants over the wide ranges of source and propagation path characteristics sampled by these tests.

The development of a seismic source summary for 122 Soviet PNE tests was described in Section 2, including how exact origin times and locations have been compiled for 69 of these explosions. In addition, exact locations and seismically based origin times with estimated accuracies of ±0.5 seconds were presented for 8 other explosions, yielding a final database of source parameters for 77 Soviet PNE tests which are accurate enough for use in highly detailed seismological investigations.

Regional seismic data recorded at the Borovoye Geophysical Observatory in Central Asia from a number of Soviet PNE tests and nearby earthquakes and mining events were analyzed in detail in Section 3. These data were processed to obtain estimates of the spectral composition of the regional phases P_n, P_g, S_n and L_g over the frequency band 0.5 to 5.0 Hz, and the resulting spectral data for the various source types were statistically analyzed to assess the level of

discrimination capability provided by data from this station. This discrimination analysis was extended in Section 4 to include an evaluation of the PIDC prototype high frequency (6-8 Hz) P_n/L_g spectral ratio discriminant using broadband, regional seismic data recorded from a number of Soviet PNE tests at both the Borovoye station and at a variety of temporary stations specifically deployed to record those explosions.

A comparison of near-regional seismic data recorded from nearby Degelen Mountain nuclear and chemical explosions was presented in Section 5, where the seismic source characteristics of these two types of underground explosions were compared and contrasted. Broadband data recorded at stations located at distances of 39 and 84 km from the Degelen test were processed to estimate the relative spectral compositions of the P, S and Rayleigh wave phases and these spectral data were used to assess the characteristics of the different explosion sources, as well as that associated with the release of tectonic strain energy which was apparantly triggered by the chemical explosion.

An analysis of the characteristics of the explosion aftershocks observed following selected Soviet PNE tests was described in Section 6, where data recorded following 13 such explosions were described and compared with corresponding data recorded from a large number of NTS underground nuclear explosions. In particular, the distributions of aftershock activity as functions of magnitude and time after these explosions were analyzed to assess their potential utility for use in onsite inspections under the CTBT.

CONVERSION TABLE

Conversion Factors for U.S. Customary to metric (SI) units of measurement.

MULTIPLY →	BY	→ TO GET
TO GET ←	BY	← DIVIDE

angstrom	1.000 000 x E -10	meters (m)
atmosphere (normal)	1.013 25 x E +2	kilo pascal (kPa)
bar	1.000 000 x E +2	kilo pascal (kPa)
barn	1.000 000 x E -28	meter^2 (m^2)
British thermal unit (thermochemical)	1.054 350 x E +3	joule (J)
calorie (thermochemical)	4.184 000	joule (J)
cal (thermochemical/cm^2)	4.184 000 x E -2	mega joule/m^2 (MJ/m^2)
curie	3.700 000 x E +1	*giga bacquerel (GBq)
degree (angle)	1.745 329 x E -2	radian (rad)
degree Fahrenheit	t_k = (t°f + 459.67)/1.8	degree kelvin (K)
electron volt	1.602 19 x E -19	joule (J)
erg	1.000 000 x E -7	joule (J)
erg/second	1.000 000 x E -7	watt (W)
foot	3.048 000 x E -1	meter (m)
foot-pound-force	1.355 818	joule (J)
gallon (U.S. liquid)	3.785 412 x E -3	meter^3 (m^3)
inch	2.540 000 x E -2	meter (m)
jerk	1.000 000 x E +9	joule (J)
joule/kilogram (J/kg) radiation dose absorbed	1.000 000	Gray (Gy)
kilotons	4.183	terajoules
kip (1000 lbf)	4.448 222 x E +3	newton (N)
kip/inch^2 (ksi)	6.894 757 x E +3	kilo pascal (kPa)
ktap	1.000 000 x E +2	newton-second/m^2 (N-s/m^2)
micron	1.000 000 x E -6	meter (m)
mil	2.540 000 x E -5	meter (m)
mile (international)	1.609 344 x E +3	meter (m)
ounce	2.834 952 x E -2	kilogram (kg)
pound-force (lbs avoirdupois)	4.448 222	newton (N)
pound-force inch	1.129 848 x E -1	newton-meter (N-m)
pound-force/inch	1.751 268 x E +2	newton/meter (N/m)
pound-force/foot^2	4.788 026 x E -2	kilo pascal (kPa)
pound-force/inch^2 (psi)	6.894 757	kilo pascal (kPa)
pound-mass (lbm avoirdupois)	4.535 924 x E -1	kilogram (kg)
pound-mass-foot^2 (moment of inertia)	4.214 011 x E -2	kilogram-meter^2 (kg-m^2)
pound-mass/foot^3	1.601 846 x E +1	kilogram-meter^3 (kg/m^3)
rad (radiation dose absorbed)	1.000 000 x E -2	**Gray (Gy)
roentgen	2.579 760 x E -4	coulomb/kilogram (C/kg)
shake	1.000 000 x E -8	second (s)
slug	1.459 390 x E +1	kilogram (kg)
torr (mm Hg, 0^0 C)	1.333 22 x E -1	kilo pascal (kPa)

*The bacquerel (Bq) is the SI unit of radioactivity; 1 Bq = 1 event/s.
**The Gray (GY) is the SI unit of absorbed radiation.

TABLE OF CONTENTS

FIGURES

FIGURES (Continued)

FIGURES (Continued)

FIGURES (Continued)

TABLES

SECTION 1
INTRODUCTION

In order to develop a comprehensive capability to discriminate the regional seismic signals produced by underground nuclear explosions from those produced by earthquakes, rockbursts and conventional mining explosions of comparable magnitude, it is first necessary to be able to define bounds on the types of signal variations which might be expected over the full ranges of source and propagation path conditions of potential interest in global monitoring of the CTBT. However, most of the empirical regional discrimination studies which have been conducted to date have focused on analyses of seismic signals recorded from underground tests conducted at the few major nuclear test sites, and these sample only limited ranges of the variables of interest. This constitutes a serious limitation in that existing theoretical simulation models have not yet proven capable of fully explaining the observed characteristics of the various proposed empirical discriminants and, therefore, their extrapolation to applications in new environments is subject to considerable uncertainty. In an attempt to overcome these limitations of previous analyses, Maxwell Technologies and the Russian Institute for Dynamics of the Geospheres (IDG) have been working on a joint research program to improve regional discrimination capability through analyses of seismic data recorded from Soviet Peaceful Nuclear Explosions (PNE) and nearby earthquakes and chemical explosions to better define the capabilities and limitations of various proposed regional discriminants. These underground nuclear explosions were widely dispersed throughout the territories of the former Soviet Union (FSU), were detonated in a wide variety of geologic emplacement media and are representative of broad ranges in explosion yield and source depth. Moreover, because of the tremendous geologic and tectonic diversity represented

within the FSU, regional data recorded from these tests sample ranges of propagation conditions that are more representative of the diversity that will be encountered in global CTBT monitoring. Thus, such data represent a unique resource for use in seismic verification studies of underground nuclear testing.

This report presents a summary of the wide variety of investigations related to Soviet PNE data which have been conducted during the course of this contract. The development of a seismic source summary for Soviet PNE tests is described in Section 2, where the different sources used to formulate the table published in the June, 1999 issue of the Bulletin of the Seismological Society of America (Sultanov et al, 1999) are discussed in detail. This is followed in Section 3 by a description of a regional discrimination analysis conducted using data recorded at the Borovoye Geophysical Observatory in Central Asia from a number of Soviet PNE tests and nearby earthquakes and mining events. In Section 4, this analysis is extended to an evaluation of the PIDC prototype high frequency P_n/L_g discriminant using broadband regional seismic data recorded from a number of Soviet PNE tests. A comparison of near-regional seismic data recorded from nearby Degelen Mountain nuclear and chemical explosions is presented in Section 5, where the seismic source characteristics of these two types of underground explosions are compared and contrasted. This is followed in Section 6 by the presentation of an analysis of the explosion aftershock characteristics observed from selected Soviet PNE tests which focuses on an assessment of their potential for use in onsite inspections under the CTBT. The report concludes with Section 7, which contains a summary and statement of conclusions regarding the implications of our analyses of Soviet PNE data with respect to global test monitoring under the CTBT.

SECTION 2

COMPILATION OF A SEISMIC SOURCE SUMMARY FOR SOVIET PEACEFUL NUCLEAR EXPLOSIONS

2.1 BACKGROUND.

During the period extending from January 1965 to September 1988, the former Soviet Union (FSU) conducted 122 peaceful nuclear explosion (PNE) tests in a variety of commercial and scientific applications. The majority of these tests can be roughly grouped into three areas of application: (1) stimulation and control of oil, gas, and mining extraction processes; (2) creation of underground storage cavities, primarily in salt; and (3) deep seismic sounding (DSS) for mapping of major crustal and upper mantle geologic structures. The remaining few events were devoted to a variety of purposes, including excavation of near-surface materials for construction projects, development of technology for obtaining transuranic elements through sequential explosions in water, and earthquake hazard studies. Most of the explosions were tamped and contained. Seven explosions were for excavation purposes and created trenches, dams, or craters. In two cases, large underground cavities created by explosions in salt (i.e. Azgir A-2-1 and A-3-1) were used for repeated explosions in air (one cavity decoupled test; Adushkin et al., 1992) and water (six low-yield explosions; Murphy et al., 1996).

The locations of the PNE tests were widely dispersed throughout the territories of the FSU. This is graphically illustrated in Figure 2-1, where the locations are shown as overlays (large squares) to a grayscale topographic map of the FSU and surrounding countries. The International Seismological Centre (ISC) seismicity database for the period 1988 to 1990 is also included as an overlay (small squares) to this map to illustrate the tectonic diversity of the PNE test environments.

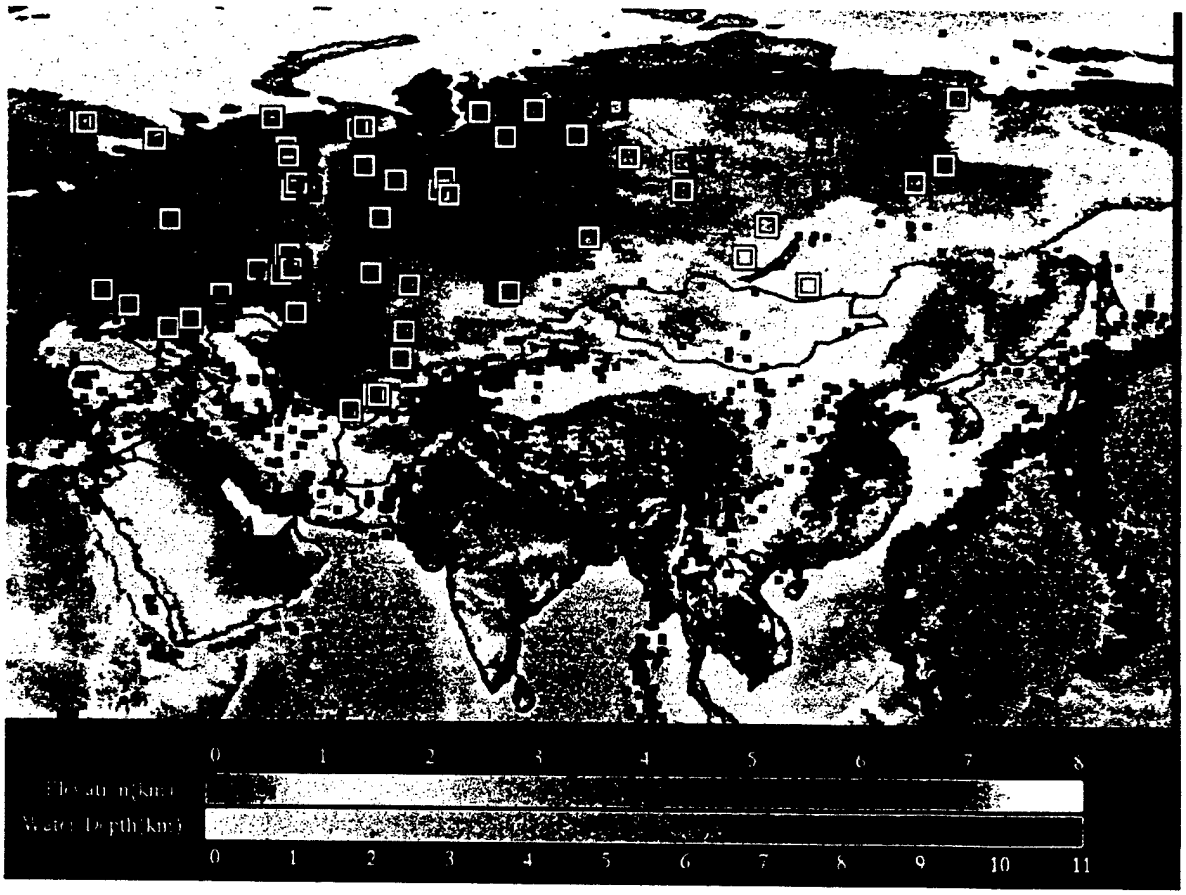

Figure 2-1. Locations of Soviet PNE events (large squares) shown as overlays to a grayscale topographic map of the former Soviet Union and surrounding countries. The larger dark squares indicate locations where multiple PNE tests were conducted. The small squares correspond to the ISC seismicity for the region for the period 1988 to 1990.

More specifically, these source locations sample the Baltic shield; the Russian, Turan, Kazakh, West Siberian, and Siberian platforms, the Caspian, Pre-Urals, and Pre-Caucasus depressions; the Baikal rift zone; and the Altai-Sayan orogenic belt. Thus, seismic data recorded from these tests represent a unique resource for studies of the variability of crust and upper mantle structures over this wide range of geophysical environments.

The Soviet PNE explosions were conducted in a variety of geologic emplacement media (e.g. sandstone/shale, limestone/dolomite, salt, clay, tuff, granite) and are representative of broad ranges in explosion yield (0.01 to 140 KT) and source depth (31 to 2860 m). The distributions of the PNE events with respect to these source variables are summarized in histogram form in Figure 2-2 where it can be

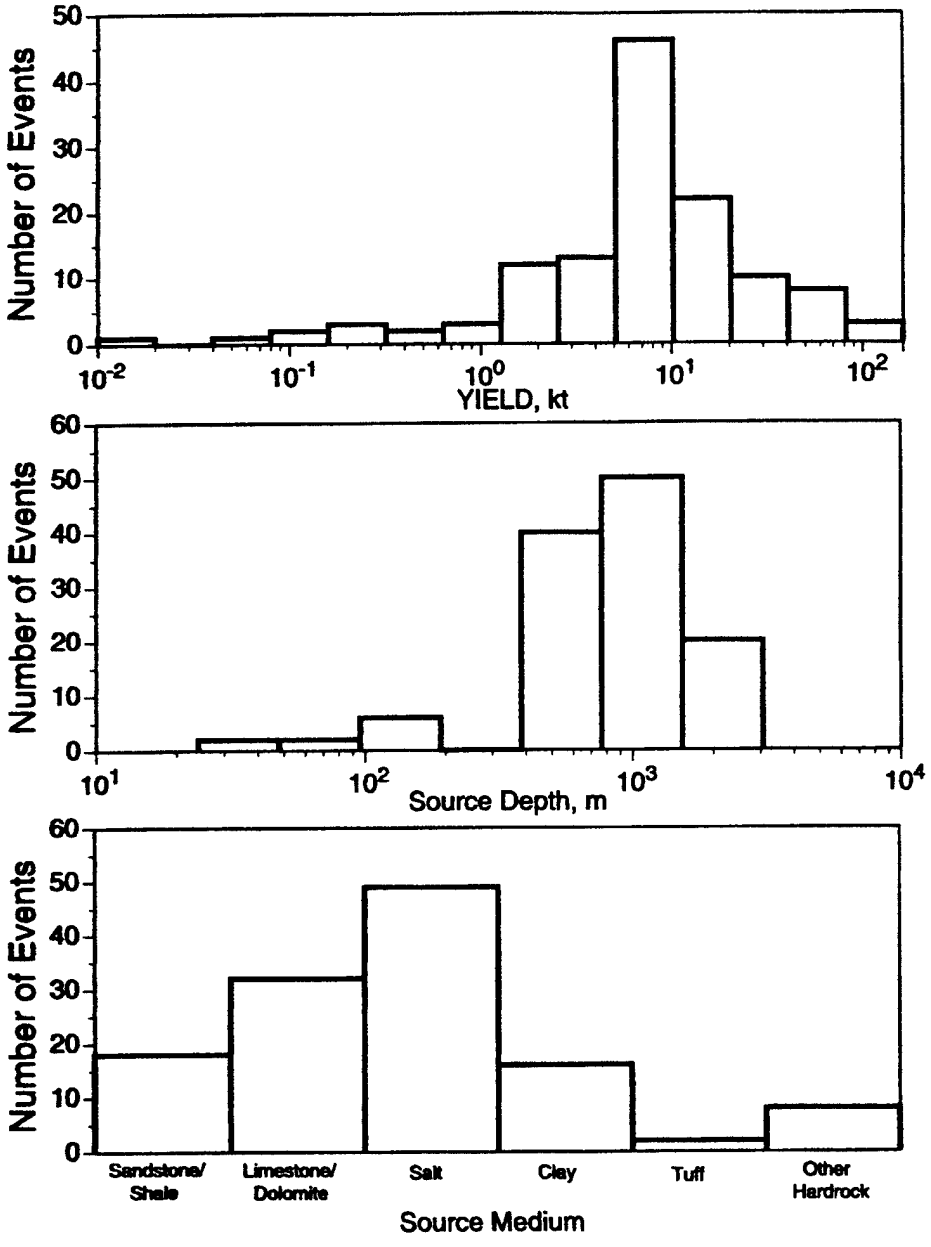

Figure 2-2. Histograms showing the distributions of the Soviet PNE events with respect to explosion yield, depth of burial, and source medium.

seen that approximately 75% of the events have yields in the 1 to 20 KT range and that nearly 60% have source depths of greater than 750 m. Thus, the majority of these PNE events are deeply overburied, low-yield explosions of the type that are of primary interest in verification studies related to seismic monitoring of the Comprehensive Test Ban Treaty. Given accurate event origin information, seismic data recorded from these Soviet PNE explosions can provide a uniquely valuable resource for use by the seismic verification community. For this reason, we have now compiled a seismic source summary for 122 Soviet PNE tests and published the results in the open literature (Sultanov et al, 1999) in a format modeled after the seismic source summary for U. S. underground nuclear explosions previously published by Springer and Kinnaman (1971, 1975). Preliminary, incomplete versions of this summary were previously published by Sultanov et al (1993) and in a summary published by the Russian Federation Ministries of Atomic Energy and Defense (1996). These prior lists provided starting points for assembling our more complete summary, which we believe incorporates all currently available, verified information regarding these tests. It should be noted that the 1996 Russian Federation summary lists 124 tests that are designated as PNE as opposed to the 122 tests included in our list. The additional 2 tests in this previous summary (04/09/71 and 12/16/74) were PNE device development tests conducted in tunnels at the seismically well-calibrated Semipalatinsk test site and are generally not regarded as operational PNE tests. Therefore, they have not been included in our list. A sample page from the Sultanov et al (1999) source summary is presented in Table 2-1, where it can be seen that the cited data are listed with variable precision. Therefore, it is necessary to qualify the accuracy of the various entries with respect to the sources of information as follows.

Table 2-1. Sample of the seismic source summary for Soviet PNE events.

Name and Date (UT)	Origin Time (UT)	Geodetic Location	Yield, kt	Depth, m	Source Medium	m_b	Comments
Horizon-3 09/29/75	11:00:00.43	69.578 N 90.337 E	7.6	834	salt	4.8	
Azgir A-3-2 03/29/76	07:00:00.23	47.897 N 48.133 E	10 (8)	986	salt	4.3	explosion in A-3-1 air-filled cavity, m_b value from Adushkin *et al.*, 1993
Azgir A-4 07/29/76	05:00:00.5	47.870 N 48.150 E	58	1000	salt	5.9	
Oka 11/05/76	03:59:59.98	61.458 N 112.860 E	15	1522	limestone	5.3	
Meteorite-2 07/26/77	17:00:00.22	69.575 N 90.375 E	15 (13)	850 (880)	salt	5.0	
Meterorite-5 08/10/77	22:00:00.10	50.955 N 110.983 E	8.5	494	granite	5.0	
Meteorite-3 08/20/77	22:00:00.78	64.108 N 99.558 E	8.5	600 (592)	tuff	5.0	
Meteorite-4 09/10/77	16:00:00.18	57.251 N 106.551 E	7.6 (7)	550 (537)	sandstone/ shale	4.8	
Azgir A-5 09/30/77	06:59:58.43	47.897 N 48.161 E	10 (9.3)	1500	salt	5.0	
Azgir A-2-3 10/14/77	06:59:59.10	47.909 N 47.912 E	0.1 (0.11)	600 (588)	salt	-	explosion in A-2-1 water-filled cavity
Azgir A-2-4 10/30/77	06:59:59.07	47.909 N 47.912 E	0.01	600 (586)	salt	-	explosion in A-2-1 water-filled cavity
Kraton-4 08/09/78	18:00:00.79	63.678 N 125.522 E	22	567	sandstone/ shale	5.6	
Kraton-3 08/24/78	18:00:00.35	65.925 N 112.338 E	22 (19)	577	limestone	5.1	
Azgir A-2-5 09/12/78	04:59:58.49	47.909 N 47.912 E	0.08	600 (584)	salt	-	explosion in A-2-1 water-filled cavity
Kraton-2 09/21/78	15:00:00.19	66.598 N 86.210 E	15 (16)	886	sandstone/ shale	5.2	
Vyatka 10/08/78	00:00:00.0	61.55 N 112.85 E	15 (13)	1545	limestone	5.2	
Azgir A-7 10/17/78	04:59:59.06	47.850 N 48.120 E	18+56	1040 970	salt	5.8	simultaneous detonation of 2 devices in same hole
Kraton-1 10/17/78	14:00:00.16	63.185 N 63.432 E	22 (23)	593	sandstone/ shale	5.5	
Azgir A-2-6 11/30/78	07:59:59.14	47.909 N 47.912 E	0.06	600 (586)	salt	-	explosion in A-2-1 water-filled cavity

2.2 ORIGIN TIME.

True origin times were obtained from automated recordings of the detonation times for 97 of the 122 PNE tests. These origin times are listed in the summary with a precision of 0.01 seconds. For an additional 17 of these explosions, the origin times have been estimated from seismic hypocenter solutions, and these are listed with a precision of 0.5 seconds. These latter estimates are based on a statistical comparison of ISC origin times and actual detonation times for 67 well-recorded PNE events for which the detonation times were automatically measured in the field. This comparison revealed that the ISC origin times for these events are early, on average, by 2.50 seconds, with an associated standard deviation of 0.38 seconds. Thus, the origin times reported in the summary for these 17 explosions were obtained by adding 2.5 seconds to their reported ISC origin times and are assumed to be accurate to within about ±0.5 seconds. Finally, there are 8 explosions for which the seismic data are inadequate for such a determination of origin time, and the origin times in these cases are listed in the summary to the nearest second based on rough, announced detonation times for these explosions.

2.3 LOCATION.

Actual locations are known for 79 of the 122 PNE events, and these are listed in the summary with a precision of 0.001°. These were estimated by geodetic means (DSS projects) or from high-resolution maps of the sites and are considered to be accurate to within 0.2 to 1.0 km. Seismic locations are listed in the summary with a precision of 0.05° for an additional 37 explosions. A comparison of seismic [ISC or U.S. Geological Survey Earthquake Data Report (EDR)] and actual locations for more than 200 explosions at the Semipalatinsk test site indicates an average seismic mislocation of 6.7 km, with a standard deviation of 4.4 km. A similar comparison for 53 Soviet PNE events with $m_b > 5.0$ indicates an average seismic

mislocation of about 7.0 km, with an associated standard deviation of 3.3 km. Thus, the seismological locations in the summary for explosions with yields greater than about 10 KT are considered to be accurate to within 5 to 10 km. The locations for the remaining 6 PNE events, which were too small to be located using teleseismic data, are listed in the summary with a precision of 0.1°. These are based on rough, geographic descriptions of the source locations and are of variable and currently unspecified accuracy.

2.4 YIELD AND DEPTH.

The explosion yields and depths of burial listed in the summary are taken from the Russian Federation summary (1996) and are considered to have nominal accuracies of about ±10% and ±5 meters, respectively. In most cases, the nuclear explosives used in the PNE tests were standard devices, the yield of which had been carefully determined during development testing at the Semipalatinsk test site. In those few cases in which previously uncalibrated devices were used, the yields were determined from in situ hydrodynamic measurements on the individual tests. Alternate, credible values from other sources of information are shown in parentheses in some cases.

2.5 SOURCE MEDIUM.

Given the complexity of the subsurface geology at a number of the PNE sites, the source media listed in the summary are only representative of the environments near source depth in some cases and, consequently, may not always provide adequate descriptions for use in assessments of variability in seismic source coupling. More detailed subsurface information is available for a number of these tests, but no comprehensive reference to these data is available at the present time.

2.6 m_b .

The m_b values listed in the summary are ISC values, except for the Magistral event of 25 June 1970 for which the EDR value is given. No teleseismic ISC or EDR m_b values were reported for 14 of these PNE events, 9 of which had yields of less than about 1 KT, and all of which had yields of less than 8 KT.

2.7 COMMENTS.

The comments are limited to the excavation explosions and those with unusual source configurations. In cases in which there were multiple explosions with horizontal offset, ΔR denotes the horizontal offsets between the explosions of the group.

2.8 CURRENT STATUS.

A seismic source summary has been published for 122 PNE tests conducted by the FSU between 1965 and 1988. Exact origin times and locations are currently available for 69 of these 122 explosions. Exact locations and seismically based origin times with estimated accuracies of ±0.5 seconds have been provided for an additional 8 explosions. Thus, the summary lists source parameters for some 77 Soviet PNE tests that are accurate enough for highly detailed seismological investigations. Hopefully, future studies encompassing analyses of satellite imagery and regional seismic data, perhaps supplemented by GPS determinations from visits to selected sites, will eventually provide accurate locations for all the other explosions in this unique data set.

SECTION 3

BOROVOYE REGIONAL DISCRIMINATION ANALYSIS

The Borovoye Geophysical Observatory is located in North Kazakhstan (53.06°N, 70.28°E) and is one of the oldest digitally recording seismic observatories in the world, having initiated digital recording in 1966. A variety of long-period and short-period seismic systems have been deployed at this station over the years (Kim and Ekström, 1996), including some relatively broadband systems which were recorded with digitization rates in the 30-40 sample/second range. Thus, dynamic range permitting, these data provide potential resolution of seismic frequency content to 10 Hz and higher. For most of the Soviet PNE tests, these Borovoye recordings represent the highest quality regional seismic data that are available for detailed analysis.

In a previous study, Murphy et al (1997) conducted a detailed analysis of the regional seismic signals recorded at the Borovoye station from 29 Soviet PNE tests located in the distance range extending from 7.2 to 19.1 degrees from the Borovoye station. The map locations of these selected explosions with respect to the Borovoye station are shown in Figure 3-1 where it can be seen that they are widely distributed throughout the territories of the former Soviet Union. Thus, their regional propagation paths to the Borovoye station sample diverse ranges of crust and upper mantle structures which can potentially provide some valuable constraints on the types of seismic characteristics which may be expected in global CTBT monitoring.

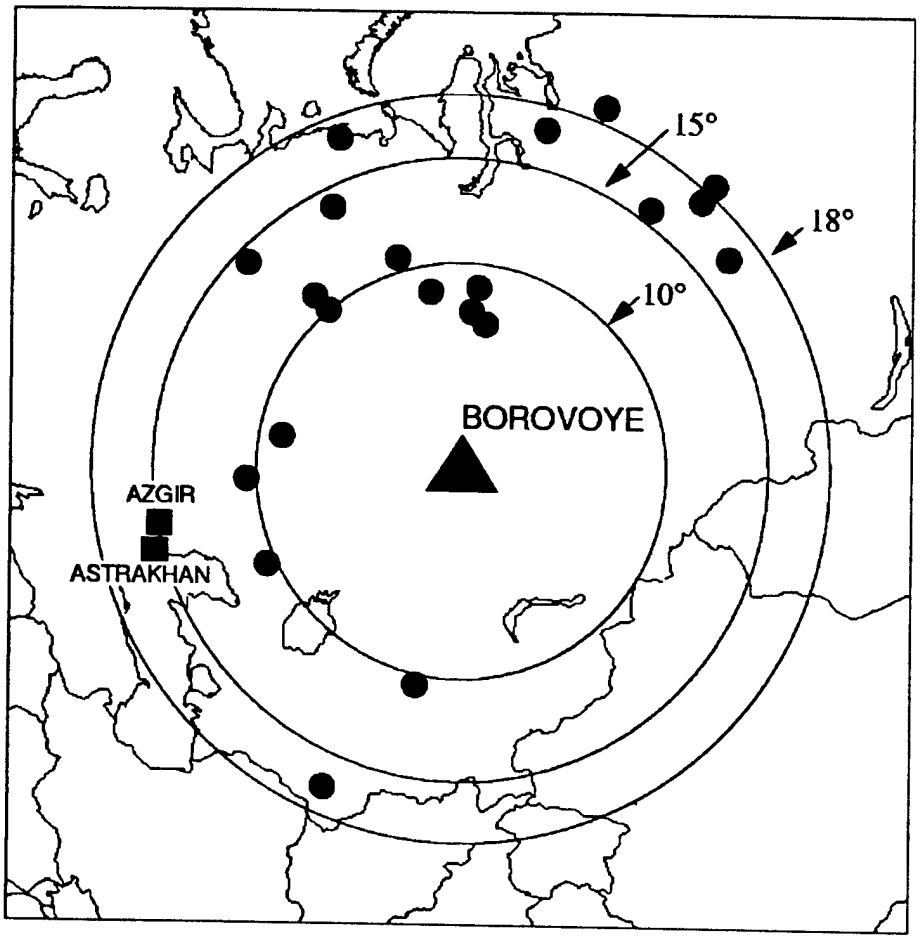

Figure 3-1. Map locations of selected Soviet PNE tests which were recorded at the Borovoye station in Kazakhstan.

The source parameters of these selected PNE events are listed in Table 3-1 where they have been divided into subsets (i.e., Groups I, II, A, B, Azgir and Astrakhan), such that the explosions in each subset are located in a fairly narrow, common distance range. Note also from Table 3-1 that, although the explosions in the Astrakhan and Azgir groups are located at distances from Borovoye which are very comparable to those of the Group A events, they were classified as separate groups in order to assess any propagation path effects which may be related to their

Table 3-1. Source characteristics of selected Soviet PNE events.

Group I ($\bar{\Delta}$ = 10.2°)						
Date	Latitude	Longitude	W,kt	h,m	Medium	Δ,°
08/15/73	42.78	67.41	6.3	600	clay	10.5
10/26/73	53.66	55.38	10	2026	dolomite	8.3
09/02/81	60.62	55.59	3.2	2088	limestone	11.0
07/21/84	51.36	53.32	13.5	846	salt	10.6
04/19/87	60.25	57.08	3.2	2015	limestone	10.4
10/03/87	47.61	56.23	8.5	1000	salt	10.5
Group II ($\bar{\Delta}$ = 8.6°)						
Date	Latitude	Longitude	W,kt	h,m	Medium	Δ,°
10/17/78	63.19	63.43	23	593	sandstone	10.7
10/04/79	60.68	71.46	21	837	clay	7.7
12/10/80	61.69	67.00	15	2485	sandstone	8.8
08/25/84	61.88	72.09	8.5	726	clay	8.9
06/18/85	60.17	72.50	2.5	2859	argillite	7.2
Group A ($\bar{\Delta}$ = 15.6°)						
Date	Latitude	Longitude	W,kt	h,m	Medium	Δ,°
04/11/72	37.37	62.00	14	1720	argillite	16.7
11/01/80	60.82	97.57	8.0	720	dolomite	16.7
09/25/82	64.31	91.83	8.5	554	gabbro	15.8
08/11/84	65.03	55.19	9.5	759	clay	14.2
09/06/88	61.36	48.09	7.5	793	dolomite	14.6
Group B ($\bar{\Delta}$ = 18.0°)						
Date	Latitude	Longitude	W,kt	h,m	Medium	Δ,°
07/26/77	69.58	90.38	13	879	salt	19.1
08/20/77	64.11	99.56	8.5	592	tuff	18.9
05/25/81	68.21	53.66	37.6	1511	clay	17.2
10/22/81	63.79	97.55	8.5	581	dolomite	17.7
09/04/82	69.21	81.65	16	960	sandstone	17.0
Astrakhan ($\bar{\Delta}$ = 15.5°)						
Date	Latitude	Longitude	W,kt	h,m	Medium	Δ,°
10/08/80	46.71	48.22	8.5	1050	salt	15.5
09/26/81	46.78	48.25	8.5	1050	salt	15.5
10/16/82	46.73	48.20	8.5	974	salt	15.5
09/24/83	46.78	48.32	8.5	1050	salt	15.4
10/27/84	46.77	48.31	3.2	1000	salt	15.5
Azgir ($\bar{\Delta}$ = 15.0°)						
Date	Latitude	Longitude	W,kt	h,m	Medium	Δ,°
09/30/77	48.14	47.85	9.3	1503	salt	15.0
07/14/79	47.81	48.10	21	982	salt	15.1
10/24/79	47.81	48.16	33	982	salt	15.0

locations within the Caspian Basin. With regard to source parameters, the data of Table 3-1 indicate that these selected explosions sample wide ranges of source media (i.e., sandstone, clay, salt, limestone/dolomite, argillite and gabbro) and source depth (i.e., 554-2859 m) and that they are predominantly low yield, overburied explosions of the type which represent the greatest challenge to seismic monitoring of the CTBT.

The Borovoye data corresponding to the selected PNE events of Table 3-1 were processed to obtain estimates of the different regional phase spectra for each event. In the first step of this processing, the data and pre-signal noise windows for each event were bandpass filtered using a Gaussian comb of filters spaced at intervals of 0.25 Hz between 0.5 and 5.0 Hz, where each filter is characterized by a Q value of 6 f_c, with f_c the filter center frequency. Filters of this type have been used by us and a number of other investigators in previous studies (Murphy *et al.*, 1989; Murphy *et al.*, 1996) and have been found to provide spectral estimates which are useful for purposes of seismic analysis. Note that, although the digitization rates for the Borovoye data are nominally high enough to support signal analyses to 10 Hz or higher, we established an upper limit of 5 Hz for the purposes of that study. This reflects our conclusion that the combination of limitations in the dynamic range of the original data, uncertainties in high frequency instrument response characteristics and the decrease in the signal-to-noise ratios with increasing frequency generally leads to a significant increase in the uncertainty associated with the reduction of the higher frequency data. For purposes of the regional phase analyses, the filter outputs for each recording were sorted into six distinct time windows and the spectral amplitudes at each center frequency were estimated by computing RMS values from the instrument-corrected filter outputs in each of the

designated windows. In the interests of simplicity and consistency, these regional phase time windows were defined in terms of apparent group velocity intervals as follows: (1) pre-signal noise, (2) $V_g > 7$ km/sec, (3) $6 < V_g < 7$ km/sec, (4) $5 < V_g < 6$ km/sec, (5) $4 < V_g < 5$ km/sec, and (6) $3 < V_g < 4$ km/sec. For purposes of subsequent discussion, these six time windows will be identified as pre-signal noise, P_n, P_{coda}, P_g, S_n, and L_g, respectively. Although there are individual cases in which refined time windows could be specified that would more precisely isolate particular regional phases of interest, this simple windowing procedure was employed throughout as a test of its potential utility for routine seismic discrimination purposes.

The resulting regional phase spectral data for this sample of Soviet PNE events were statistically analyzed in detail by Murphy et al (1997) to define their dependencies on the various explosion source and propagation path variables, and a simple model was developed for estimating the spectral compositions of the different regional phases over the sampled ranges of these variables. One of the more interesting results of this spectral analysis was the identification of a number of explosion signals which appear to be somewhat anomalous with respect to some proposed regional discriminants such as that based on the high frequency S/P spectral amplitude ratio. One example of such an anomalous explosion signal is provided by the Borovoye recording of the Soviet PNE event of 6/18/85 ($\Delta = 7.2°$) which was detonated with a yield of 2.5 KT at a depth of 2859 m in limestone. The unfiltered vertical component Borovoye recording of this explosion is shown in Figure 3-2, together with corresponding outputs of narrowband Gaussian filters ($Q = 6f_c$) with filter center frequencies, f_c, ranging from 0.5 to 10 Hz. Also shown on this plot are dashed vertical lines denoting the group arrival times associated with

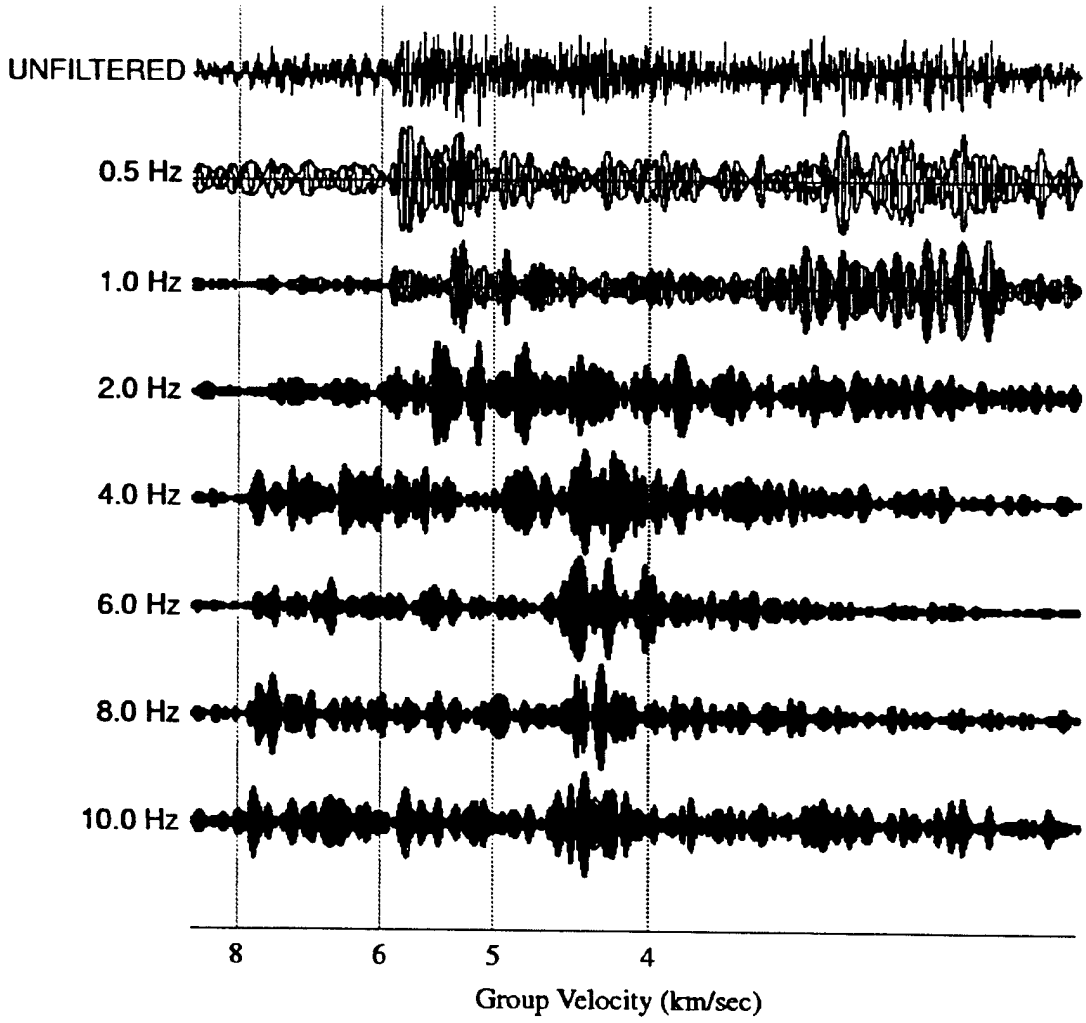

Figure 3-2. Comparison of broadband vertical component seismogram and associated bandpass filter outputs derived from the Borovoye station recording of the Soviet PNE event of 6/18/85, $\Delta = 7.2°$.

various apparent velocities of propagation between the source and the station. Note that if we associate a group velocity of 5 km/sec with the approximate boundary between "P" and "S" arrivals, then the high frequency ($f > 2$ Hz) S/P ratios in this case are significantly greater than 1.0, which is inconsistent with some generalized discrimination criteria which have been proposed for underground nuclear explosions. This example once again points out the need for careful calibration of propagation path effects and has motivated our comparative study of the seismic

signal characteristics of earthquakes and other source types which have occurred in the vicinity of these Soviet PNE tests.

In an attempt to more carefully assess regional discrimination at Borovoye, data recorded at that station from the 29 Soviet PNE events have now been supplemented with data recorded from 22 PIDC REB events located within 20 degrees of Borovoye. The map locations of these selected REB events with respect to the previously analyzed PNE events are shown in Figure 3-3, where it can be

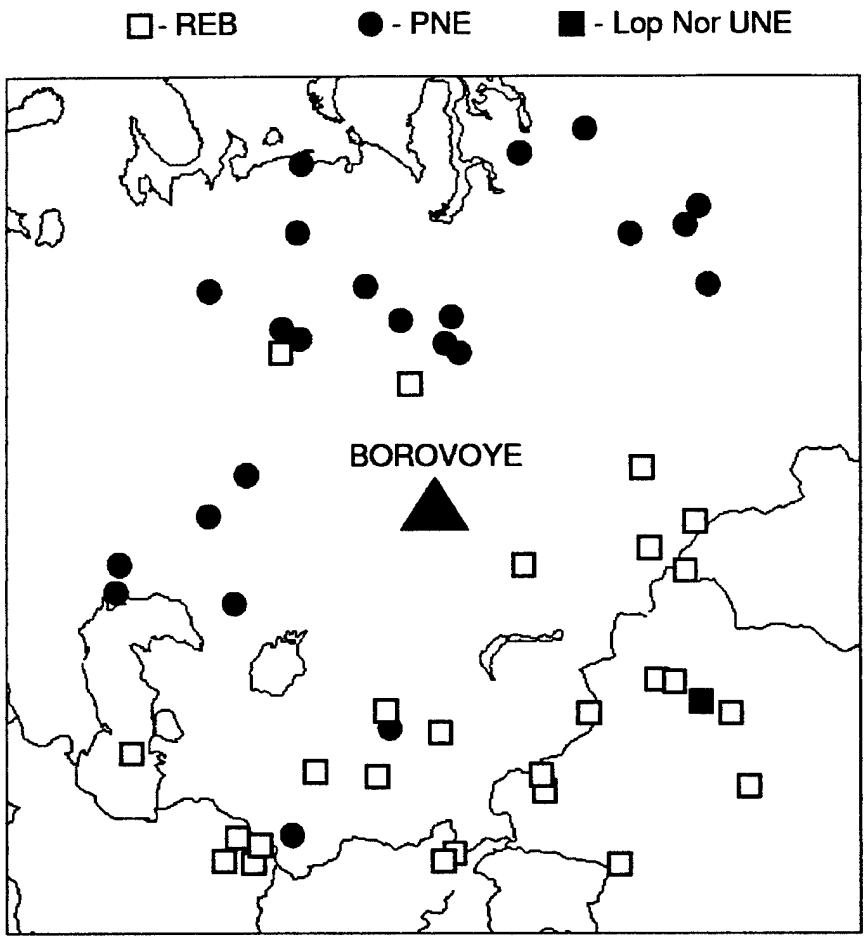

Figure 3-3. Map locations of Soviet PNE tests and selected REB events located within 20° of the Borovoye station in Kazakhstan.

seen that the geographical distributions of the two sets of events are sub-optimal in that most of the PNE events are located north of the station, while most of the REB events are located south of the station. This is unfortunate, but it is an unavoidable consequence of the essentially aseismic nature of the stable platform regions to the north of Borovoye. The source characteristics of these selected REB events are summarized in Table 3-2, where it is noted that, while most of these events are presumably natural earthquakes, two of them are Lop Nor nuclear explosions and

Table 3-2. Source parameters of selected regional REB events recorded at the Borovoye station.

Date	Origin Time	Latitude	Longitude	Δ°	mb	Comments
09/14/95	04:24:04.2	53.67	86.90	10.0	4.5	
01/05/95	12:46:01.3	59.52	56.31	10.1	4.4	Mine collapse
04/18/97	10:16:55.9	43.09	67.20	10.2	4.0	
09/18/97	14:31:45.5	49.92	86.21	10.4	4.2	
08/19/95	20:28:06.3	42.33	70.65	10.8	4.6	
11/01/95	12:29:33.6	42.93	80.26	12.2	4.9	
02/11/96	14:46:56.2	50.58	89.86	12.4	4.0	
03/12/96	18:43:40.8	48.48	88.39	12.4	5.2	
08/29/97	02:16:30.6	40.14	66.74	13.2	4.4	
05/02/95	11:48:08.4	43.87	84.89	13.4	5.3	
12/29/96	18:03:45.1	40.25	63.02	13.7	3.9	
01/09/96	06:27:55.7	43.68	85.72	13.9	4.8	
03/19/98	13:51:30.4	39.92	76.68	13.9	5.1	
10/17/97	17:35:21.2	39.42	76.79	14.4	3.9	
03/18/95	18:02:34.7	42.46	87.30	15.6	4.9	
05/15/95	04:05:59.6	41.63	88.87	17.0	5.7	Lop Nor UNE
08/17/95	00:59:59.3	41.60	88.86	17.0	5.5	Lop Nor UNE
08/09/97	17:05:28.8	36.54	60.38	17.9	4.1	
02/23/97	13:22:41.4	36.68	58.89	18.2	4.0	
10/29/95	06:27:20.8	39.60	51.90	18.4	5.0	
11/09/95	05:10:29.3	35.64	59.87	18.9	4.9	
10/15/97	20:30:52.2	35.65	80.75	18.9	4.4	

one of them is a documented mine collapse event in the Urals. It can be seen from Table 3-2 that these events encompass an epicentral distance range extending from about 10 to 19 degrees and a range of m_b extending from 3.9 to 5.7, both of which overlap substantially with the corresponding ranges for the PNE events. Of course, the REB locations in this table are based on the limited data provided by the presently incomplete IMS network and, therefore, it is appropriate to question whether they are accurate enough for our comparison purposes. In an attempt to address this issue, we relocated these events by adding the observed first arrival times of the Borovoye station to the original REB data sets. The average resulting change in epicentral location was found to be less than 14 km, with a maximum difference of 32 km. Therefore, we have tentatively concluded that these REB locations are adequate for the purposes of the present investigation.

Samples of the vertical component data recorded at the Borovoye station from several of the selected REB events are displayed in Figure 3-4, where it can be seen that the generalized S/P amplitude ratios on these broadband recordings are highly variable from event to event. Corresponding data from all 22 REB events were processed using exactly the same procedures which were applied to the Borovoye PNE data, as described above, to obtain instrument-corrected, regional phase spectral estimates for each of the designated regional phases. These spectral data were then used to calculate L_g/P_n, L_g/P_g, S_n/P_n, S_n/P_g and L_g discriminant ratios corresponding to each PNE and REB event recording. Since it has been demonstrated in numerous previous studies that S/P type phase ratio discriminants work best at higher frequencies, the interphase ratio values were logarithmically averaged over the frequency band 2 to 5 Hz. The L_g discriminant ratio, on the other hand, was patterned after that initially proposed by Murphy and Bennett (1982),

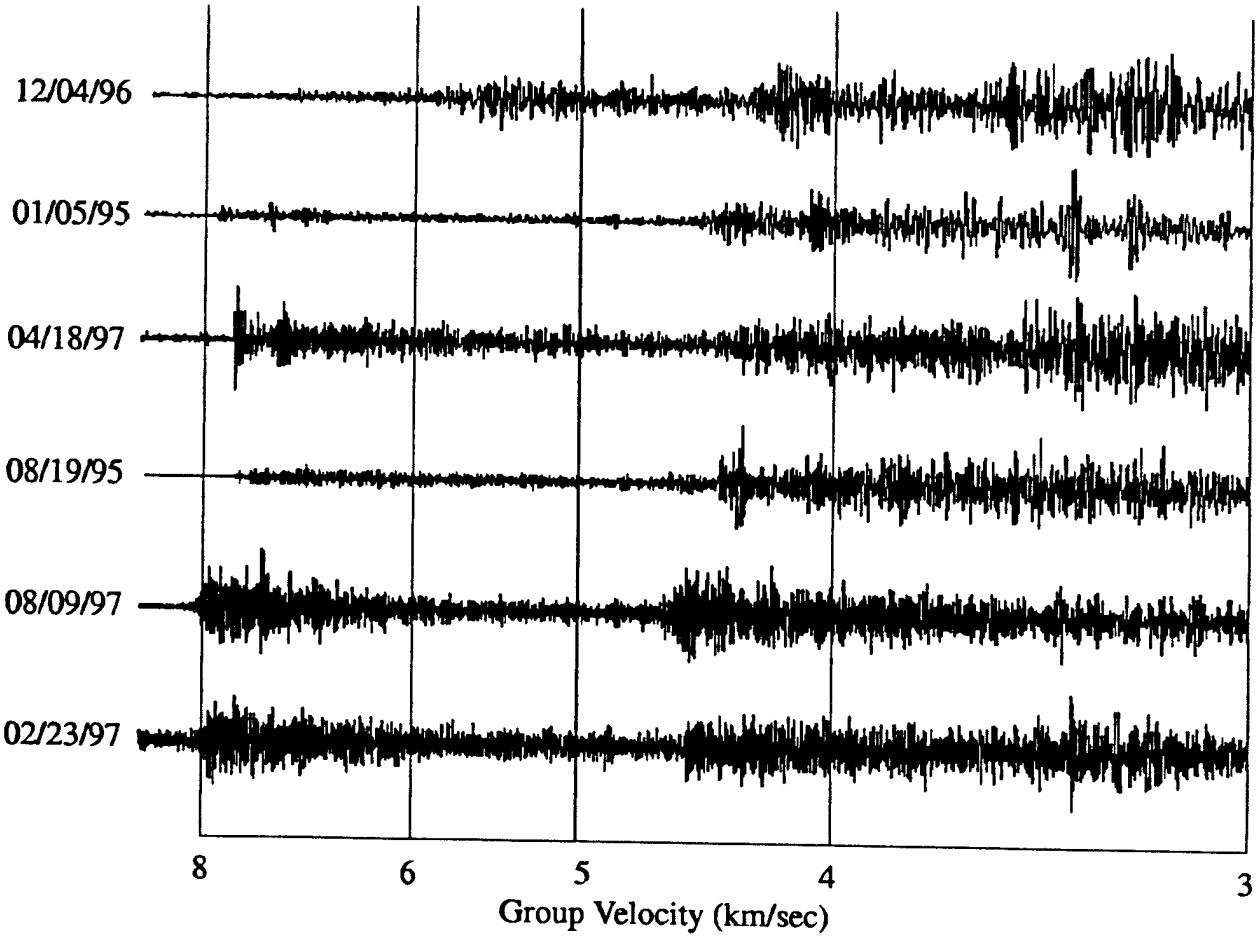

Figure 3-4. Vertical component regional signals recorded at Borovoye from selected REB events located in the vicinity of previous Soviet PNE events.

and was defined as the ratio of the average L_g spectral amplitude level in the 0.50 to 1.25 Hz band to that in the 2.0 to 5.0 Hz band.

Review of these various spectral ratio data revealed that they all showed trends with epicentral distance (Δ) and magnitude (m_b). Consequently, for each ratio type, the PNE and REB spectral ratio values were separately analyzed in multivariate regression analyses in which the data for each phase ratio type p were fit to a functional relation of the form

$$Rp = Kp \cdot 10^{n_p m_b} \cdot \Delta^{m_p} \tag{2.1}$$

The regression analysis results for the L_g/P_n spectral ratio data are shown in Figures 3-5 and 3-6 for both the PNE and REB data sets, where the observed ratio data have been normalized to the sample mean distance and magnitude levels (i.e. $\Delta = 12.5°$, $m_b = 4.6$), respectively for display purposes. It can be seen that the variations with both distance and magnitude are quite similar for the two event groups in this case. This was found to be true for all the other phase spectral ratios as well and, consequently, the statistically derived n_p and m_p scaling exponents for the PNE and REB samples were averaged for each spectral ratio type and these average exponents were used to scale all the observed spectral ratio values to the sample mean distance and magnitude as follows:

L_g: $$\frac{Lg\,(0.50-1.25Hz)}{Lg\,(2.00-5.00Hz)} \bullet 10^{-0.40(m_b-4.6)} \bullet \left(\frac{\Delta}{12.5}\right)^{-0.40} \tag{2.2}$$

L_g/P_n: $$L_g/P_n\,(2.00-5.00Hz) \bullet 10^{0.20(m_b-4.6)} \bullet \left(\frac{\Delta}{12.5}\right)^{2.5} \tag{2.3}$$

L_g/P_g: $$L_g/P_g\,(2.00-5.00Hz) \bullet 10^{0.20(m_b-4.6)} \bullet \left(\frac{\Delta}{12.5}\right)^{1.0} \tag{2.4}$$

S_n/P_n: $$S_n/P_n\,(2.00-5.00Hz) \bullet 10^{0.20(m_b-4.6)} \bullet \left(\frac{\Delta}{12.5}\right)^{2.0} \tag{2.5}$$

S_n/P_g: $$S_n/P_g\,(2.00-5.00Hz) \bullet 10^{0.20(m_b-4.6)} \bullet \left(\frac{\Delta}{12.5}\right)^{0.5} \tag{2.6}$$

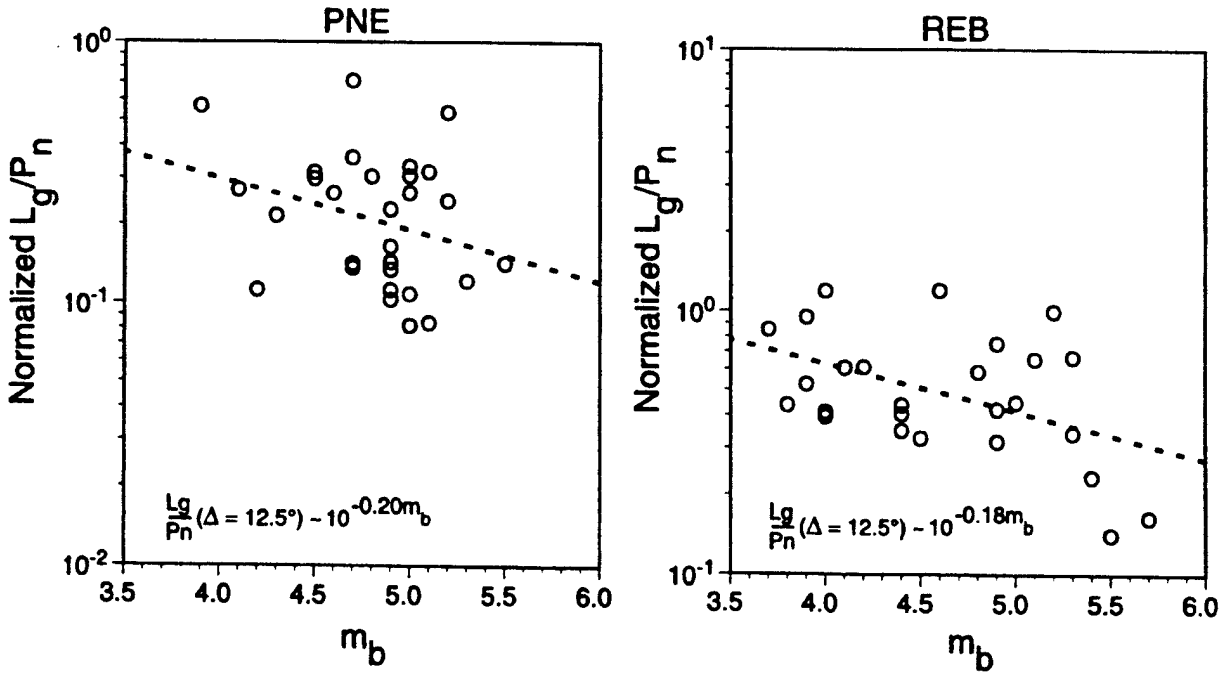

Figure 3-5. Comparison of magnitude dependence of the distance normalized L_g/P_n spectral ratios (2.0 – 5.0 Hz) for the Borovoye PNE and REB events.

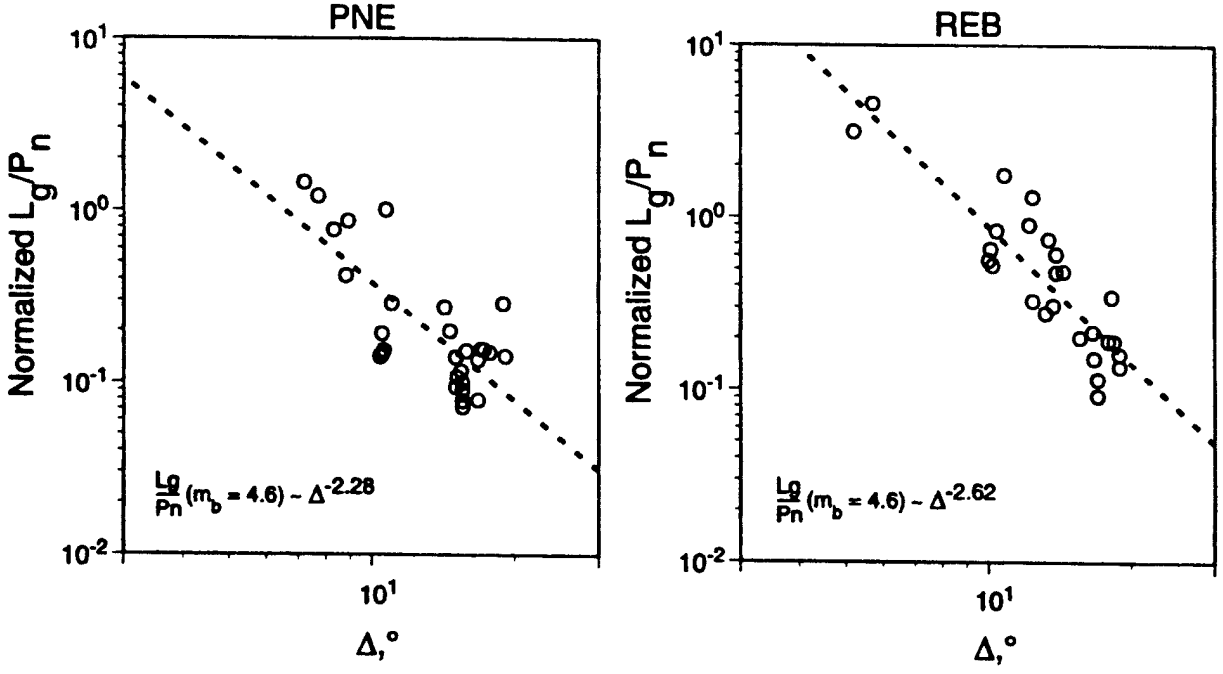

Figure 3-6. Comparison of distance dependence of the magnitude normalized L_g/P_n spectral ratios (2.0 – 5.0 Hz) for the Borovoye PNE and REB events.

Note that since the PNE and REB data are normalized in exactly the same way for each phase ratio type, no average bias between event groups is introduced by this scaling procedure.

The resulting normalized discriminant values for the L_g/P_n spectral ratios are plotted as a function of m_b in Figure 3-7, where it can be seen that there is some average separation between the underground nuclear and other source types, with the discriminant values for the Lop Nor underground nuclear explosions falling very close to the mean of the Soviet PNE data. However, it is also obvious that there is considerable intermixing of the individual spectral ratio values for the

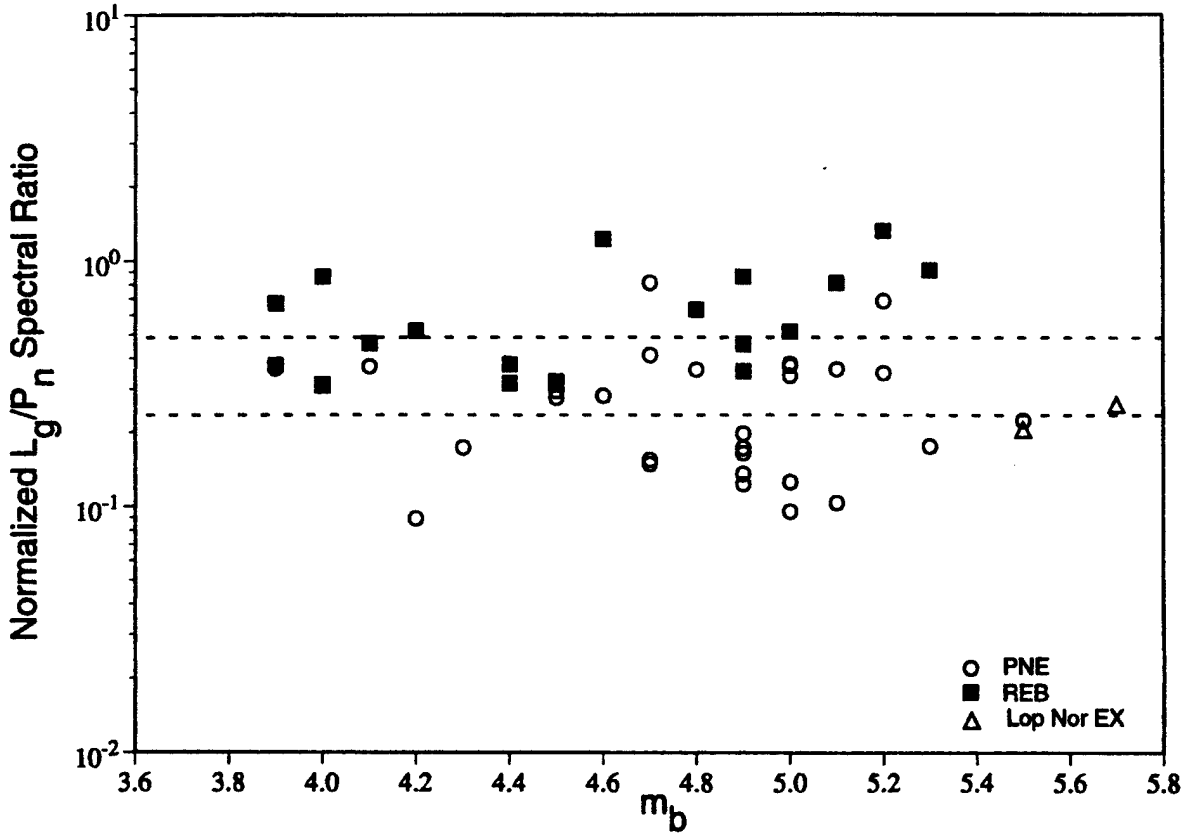

Figure 3-7. Comparison of normalized L_g/P_n spectral ratio values (2.0 – 5.0 Hz) for Borovoye PNE and REB recordings. The upper and lower dashed lines denote the logarithmic means of the REB and PNE populations, respectively.

different source types which diminishes the reliability of this discriminant. Examination of the geographical distribution of those PNE events with discriminant ratio values which mix into the REB population (i.e. normalized L_g/P_n ratio values > 0.3 in Figure 3-7) indicate that they all fall in a rather narrow azimuth window to the north of the Borovoye station. This fact is documented in Figure 3-8 where the map locations of the PNE events corresponding to these anomalous L_g/P_n ratio values have been circled. The pronounced geographical

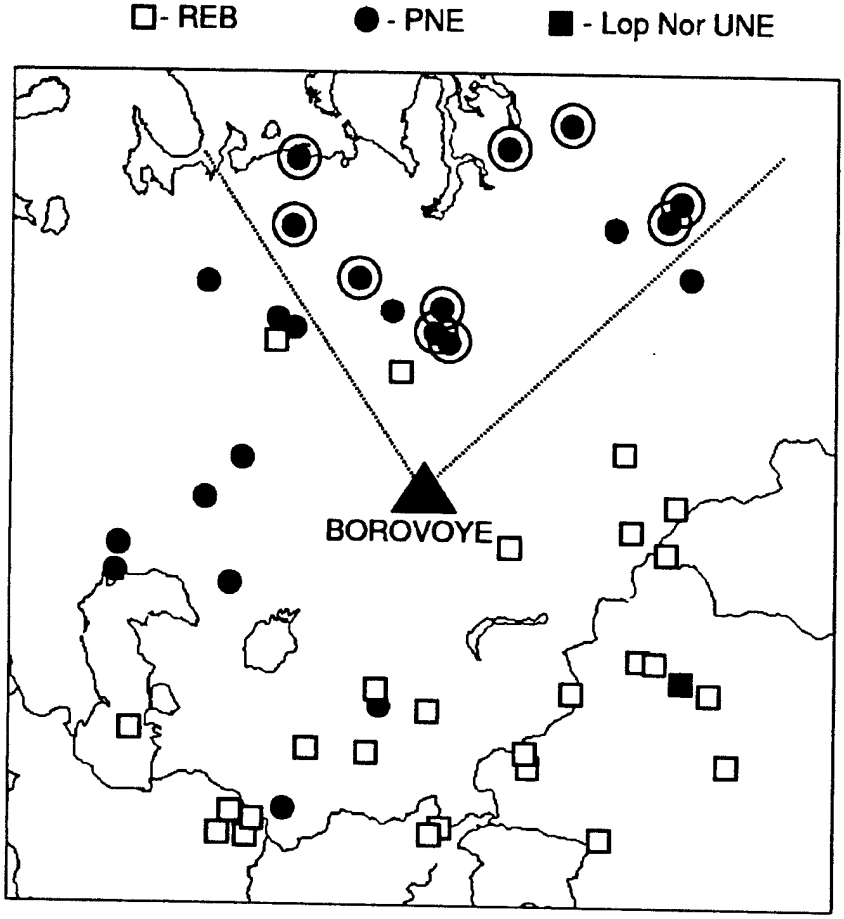

Figure 3-8. Map locations of Soviet PNE tests and selected REB events located within 20° of the Borovoye station in Kazakhstan. The circled PNE events are those which have L_g/P_n spectral ratio values at Borovoye which mix into the earthquake population.

concentration of these high explosion ratio values suggests that propagation path effects are the primary cause of the anomalous discrimination results. Unfortunately, however, this apparent variability does not seem to correlate with any mapped crustal structure variation in the region, and the essentially aseismic nature of this region makes it difficult to empirically assess expected discrimination capability. In any case, these results indicate that any proposed L_g/P_n spectral ratio discriminant will have to be carefully calibrated for application to previously untested sites, at least for applications employing the frequency band below 5 Hz.

Corresponding results for the L_g/P_g, S_n/P_n and S_n/P_g spectral ratios are shown in Figures 3-9 through 3-11, where it can be seen that the average separations of the source types are generally smaller than that found for the L_g/P_n spectral ratio, with considerable intermixing of the two event populations in all cases. As has been noted previously (Murphy et al, 1997), the ratios computed with respect to P_g generally show less scatter than those computed with respect to P_n. However, comparison of Figures 3-7 and 3-10 and Figures 3-9 and 3-11 indicate that the ratios computed with respect to P_n provide somewhat better event discrimination capability as is illustrated by the results for the two Chinese Lop Nor underground nuclear tests. Moreover, the S_n spectral ratio discriminants are clearly inferior to the corresponding L_g spectral ratio discriminants, and they provide very little identification capability with respect to these two populations of events.

Somewhat surprisingly, it was found that the best separation of Borovoye PNE and REB events was provided by the L_g spectral ratio discriminant. This robustness is documented in Figure 3-12 where it can be seen that the mean values of this

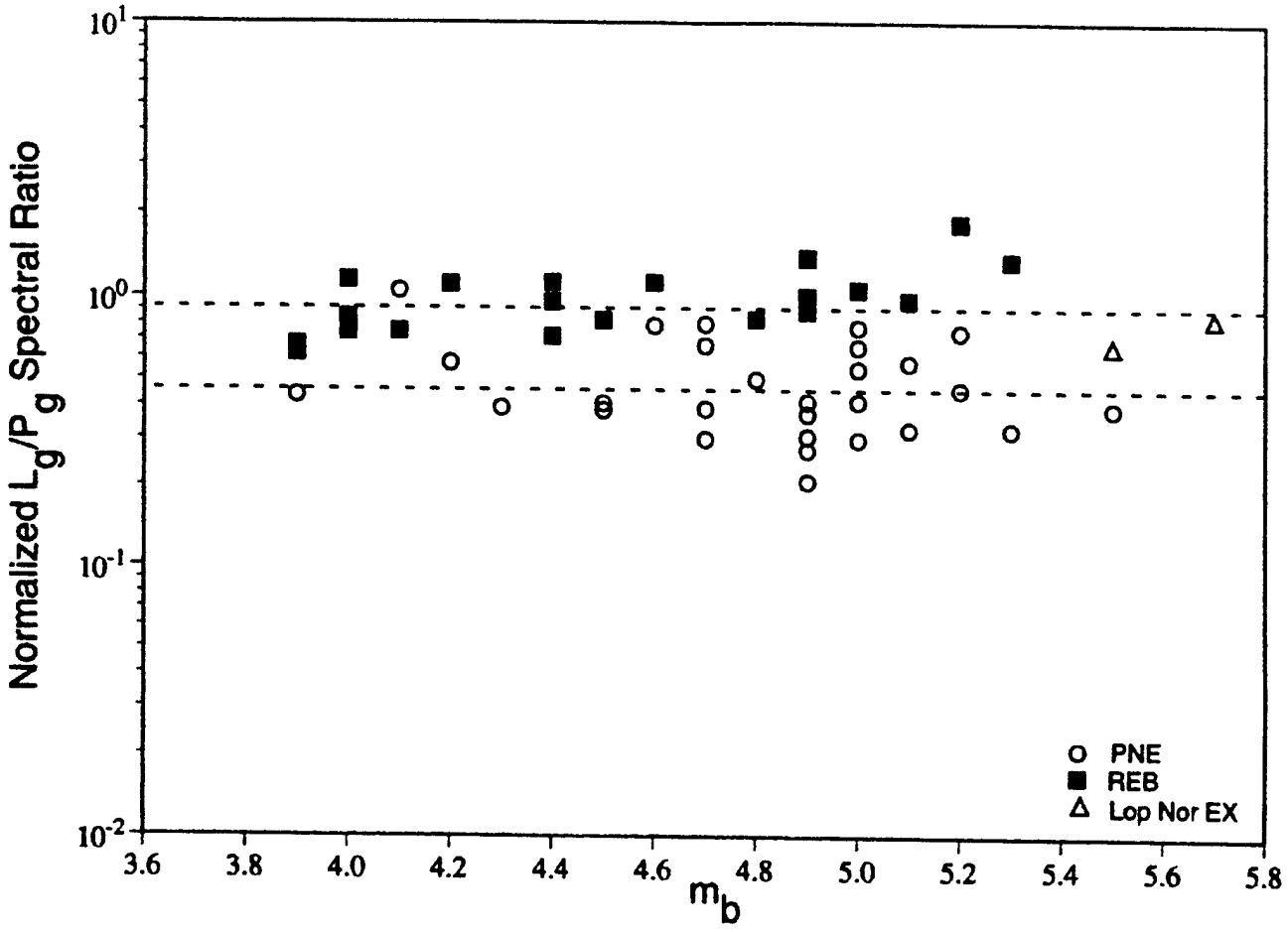

Figure 3-9. Comparison of normalized L_g/P_g spectral ratio values (2.0 – 5.0 Hz) for Borovoye PNE and REB recordings. The upper and lower dashed lines denote the logarithmic means of the REB and PNE populations, respectively.

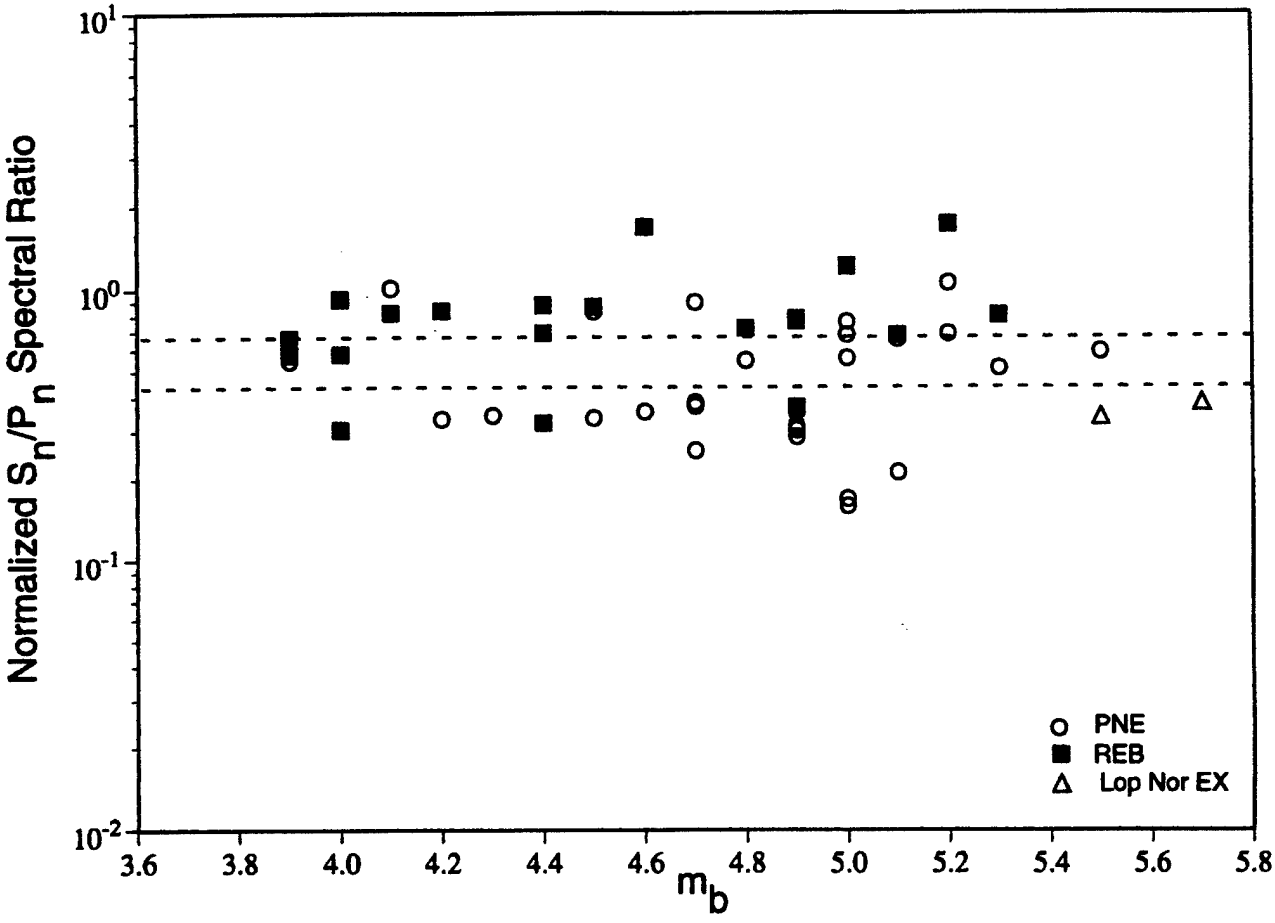

Figure 3-10. Comparison of normalized S_n/P_n spectral ratio values (2.0 – 5.0 Hz) for Borovoye PNE and REB recordings. The upper and lower dashed lines denote the logarithmic means of the REB and PNE populations, respectively.

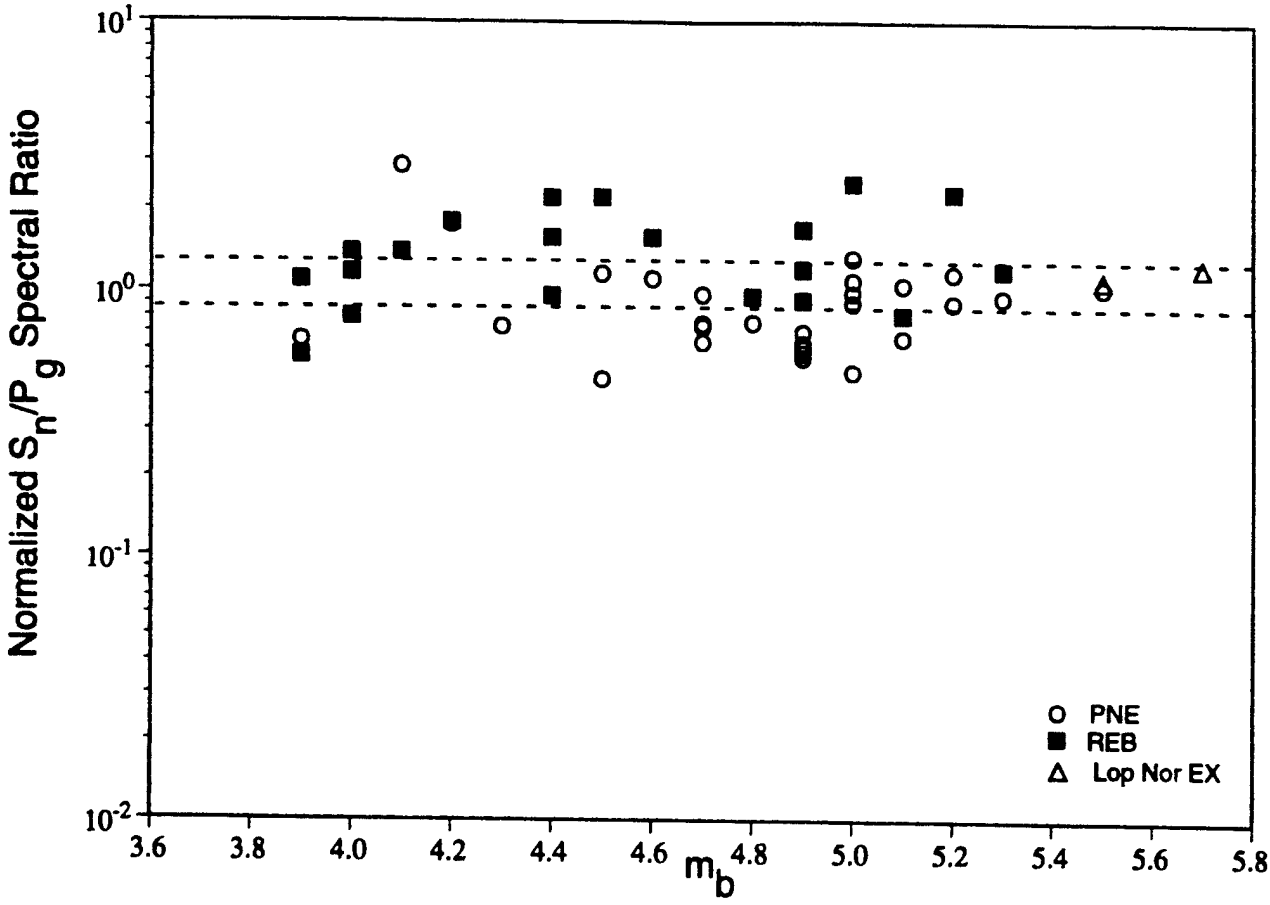

Figure 3-11. Comparison of normalized S_n/P_g spectral ratio values (2.0 – 5.0 Hz) for Borovoye PNE and REB recordings. The upper and lower dashed lines denote the logarithmic means of the REB and PNE populations, respectively.

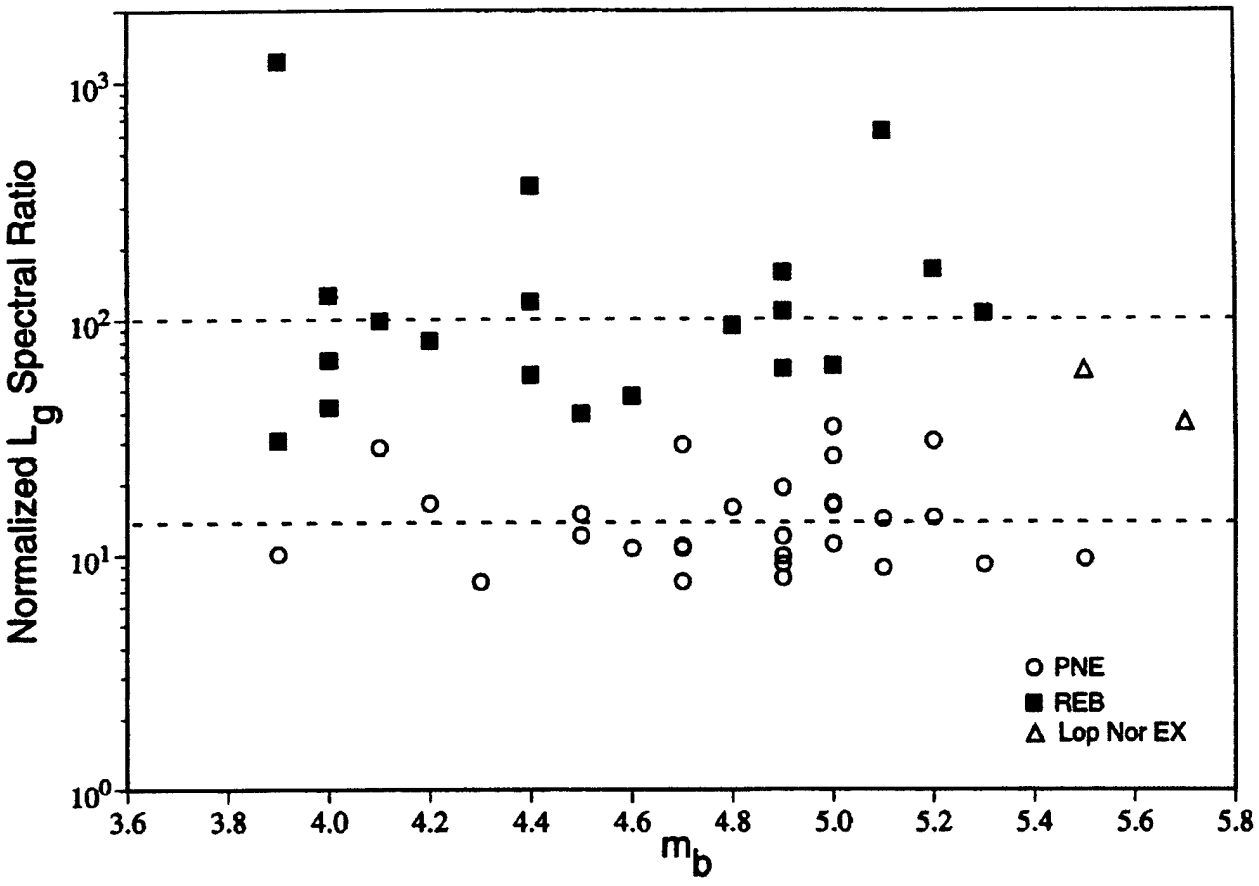

Figure 3-12. Comparison of normalized L_g spectral ratio values (0.50 – 1.25 Hz / 2.00 – 5.00 Hz) for Borovoye PNE and REB recordings. The upper and lower dashed lines denote the logarithmic means of the REB and PNE populations, respectively.

discriminant for the two event groups are separated by nearly a full order of magnitude, with very little intermingling of the two populations. Particularly noteworthy is the fact that the Urals mine collapse, which is difficult to discriminate using the interphase spectral ratios of Figures 3-7 and 3-9 through 3-11, has the largest L_g spectral ratio value of the events analyzed, lying nearly two orders of magnitude above the average PNE value. Unfortunately, the sense of the observed difference is opposite to that found by Murphy and Bennett (1982) for NTS explosions, which indicates that the performance of this discriminant can be expected to vary significantly as a function of source and propagation path conditions. It follows that, in the absence of a quantitative theoretical model which can be used to predict this variability, it will be necessary to empirically calibrate any such L_g spectral ratio discriminant on a station by station and region by region basis. However, it may well be worth such an effort in regions where the separation of source types is as powerful as that shown in Figure 3-12. Clearly, additional research is needed to develop a quantitative theoretical understanding of the behavior of this discriminant.

SECTION 4

APPLICATION OF THE PIDC HIGH FREQUENCY P_n/L_g DISCRIMINANT TO REGIONAL SEISMIC DATA RECORDED FROM SOVIET PNE TESTS

The Borovoye discrimination analysis summarized in the previous section was limited to the extent that it focused on data from a single station at frequencies below 5 Hz. In fact, it has long been recognized that higher frequency data can often provide more robust discrimination capability, and the prototype PIDC regional discriminant relies heavily on P_n/L_g spectral ratio data in the 6-8 Hz band (Fisk et al, 1999). Unfortunately, it is not always possible to achieve adequate signal to noise ratios in this high frequency band for small events recorded at epicentral distances outside the near-regional range and, consequently, it was necessary to limit the Borovoye analysis to frequencies less than 5 Hz in order to obtain a homogeneous sample. However, subsets of the Borovoye PNE data were recorded with usable signal to noise ratios in the 6-8 Hz band, and these data have been reprocessed to provide test data which can be used to further evaluate the PIDC high frequency P_n/L_g discriminant. In addition, although the Borovoye station was the only Soviet station which provided direct digital data for most Soviet PNE tests, a number of temporary stations were also deployed on selected tests which recorded analog data at high enough recording speeds to be readily digitized at rates compatible with frequency resolution up to at least 10 Hz. Therefore, these data have also been digitized and processed to provide supplemental data suitable for testing the prototype PIDC regional discriminant.

The map locations of the Soviet PNE events for which high frequency (6-8 Hz) P_n/L_g spectral ratio discriminant values have now been estimated are shown in Figure 4-1, where it can be seen that they are fairly widely distributed throughout the territories of the FSU. The source parameters of these explosions are listed in

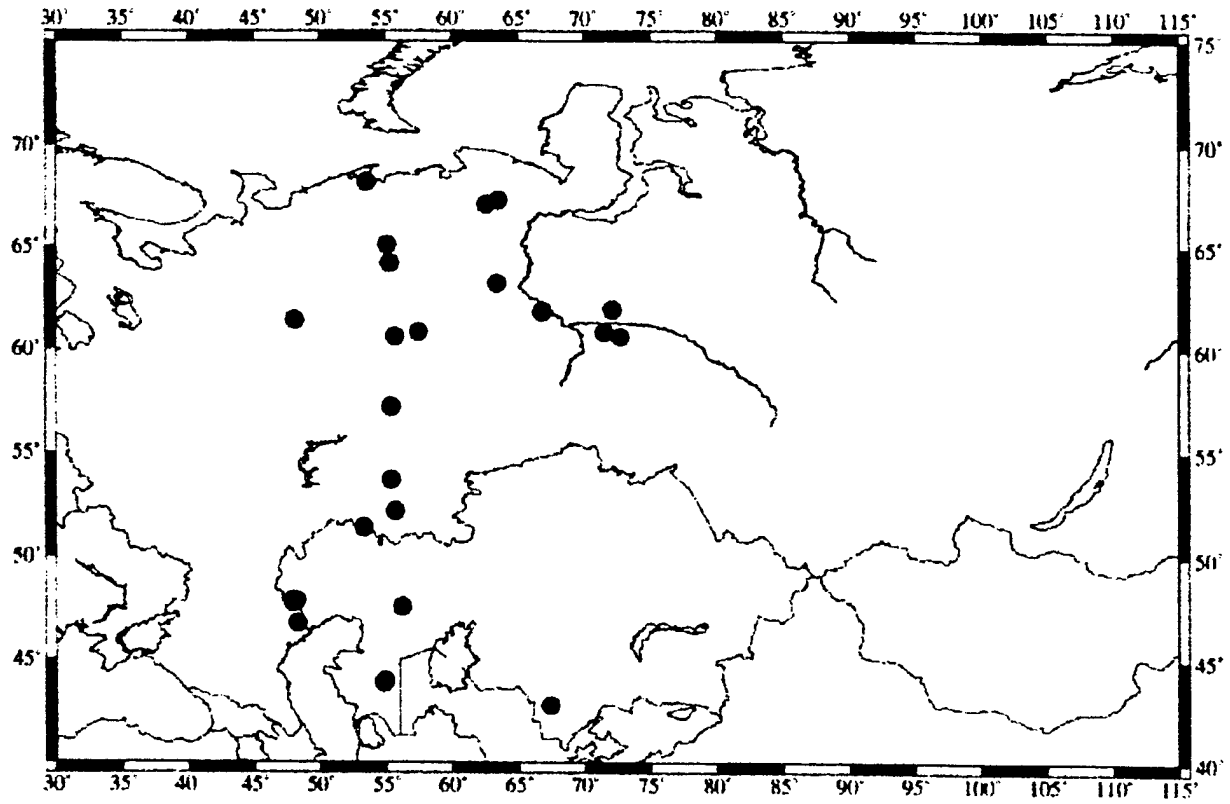

Figure 4-1. Map locations of Soviet PNE events for which high frequency (6-8 Hz) Pn/Lg spectral ratio discriminant values have been estimated from recorded regional seismic data.

Table 4-1 where it is indicated that they encompass a range of source media (salt, limestone, sandstone/shale, clay, chalk), with yields ranging from 1.1 to 80 KT and scaled depths ranging from 115 to 2107 m/kt$^{1/3}$. Broadband vertical component regional signals recorded at various temporary stations from a representative set of these Soviet PNE tests are displayed in Figure 4-2, where it can be seen that some of them show evidence of strong S_n and L_g phases which are comparable in amplitude to those of the associated P phases. Bandpass filtered (6-8 Hz) vertical component signals corresponding to these same recordings are shown in Figure 4-3. Note that even in this relatively high frequency band, some of these explosion recordings show evidence of surpisingly large amplitude S_n and L_g phases, contrary

Table 4-1. Seismic source characteristics of Soviet PNE events used in the PIDC regional discrimination analysis.

DATE	LAT,N	LONG, E	W, kt	h, m	$h/w^{1/3}$,$m/kt^{1/3}$	MEDIUM
04/22/66	47.83	47.94	1.1	161	156	Salt
07/01/68	47.91	47.91	27	597	199	Salt
09/02/69	57.22	55.39	7.6	1212	616	Limestone
09/08/69	57.22	55.42	7.6	1208	614	Limestone
12/06/69	43.87	54.80	30	407	131	Chalk
06/25/70	52.20	55.70	2.3	702	532	Salt
12/12/70	43.85	54.80	80	497	115	Chalk
07/02/71	67.28	63.47	2.3	542	411	Sandstone/Shale
07/10/71	64.17	55.27	2.3	465	352	Clay
04/11/72	37.35	62.05	15	1720	697	Limestone
08/15/73	42.78	67.41	6.3	600	325	Clay
10/26/73	53.65	55.40	10	2026	940	Limestone
08/29/74	67.09	62.63	7.6	583	297	Sandstone/Shale
09/30/77	47.90	48.16	10	1500	696	Salt
10/17/78	47.85	48.12	74	1040	248	Salt
07/14/79	47.88	48.12	21	982	356	Salt
10/04/79	60.68	71.46	22	837	299	Clay
10/24/79	47.85	48.14	33	980	306	Salt
10/08/80	46.76	48.28	8.5	1050	514	Salt
12/10/80	61.75	66.75	15	2485	1008	Sandstone/Shale
05/25/81	68.20	53.50	37.6	1511	451	Sandstone/Shale
09/02/81	60.60	55.70	3.2	2088	1417	Limestone
10/16/82	46.76	48.25	8.5	947	464	Salt
07/21/84	51.36	53.31	15	846	343	Salt
08/11/84	65.05	55.10	8.5	759	372	Clay
08/25/84	61.90	72.10	8.5	726	356	Clay
06/18/85	60.60	72.70	2.5	2860	2107	Sandstone/Shale
04/19/87	60.80	57.50	3.2	2055	1395	Limestone
10/03/87	47.60	56.20	8.5	1002	491	Salt
09/06/88	61.36	48.09	8.5	820	402	Anhydrite

to what might be expected based on the predictions of most simple models of the explosion source.

The 6-8 Hz P_n/L_g discriminant ratio values determined from the broadband regional recordings of these selected Soviet PNE events are plotted in Figure 4-4, where they are compared with the corresponding mean and 2σ bounds on the large

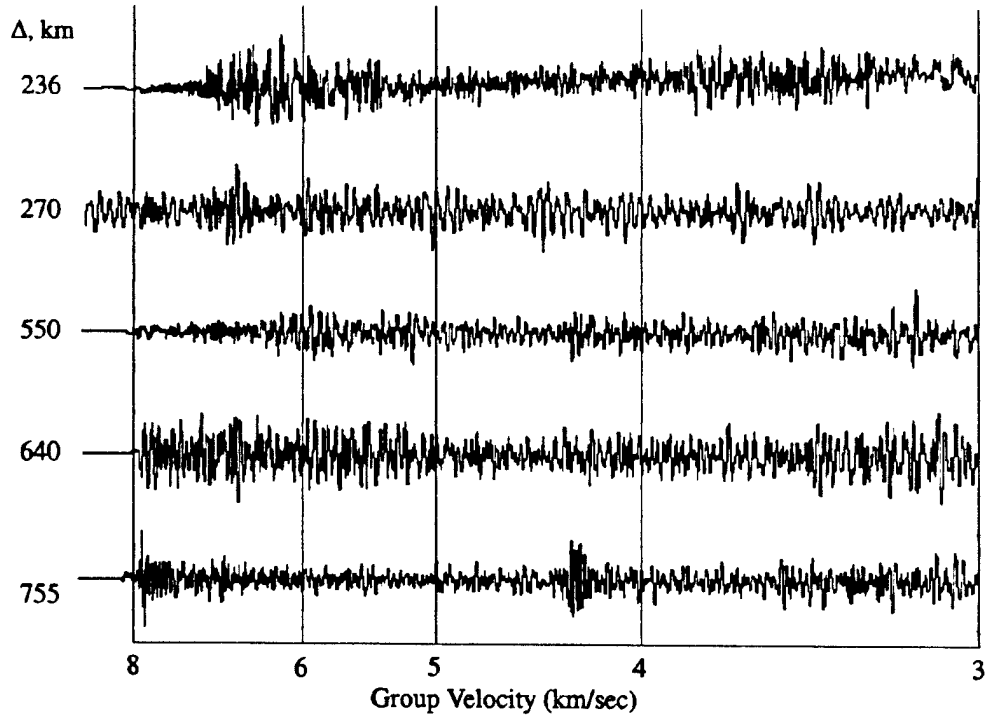

Figure 4-2. Broadband vertical component regional signals recorded at various temporary stations from selected Soviet PNE events.

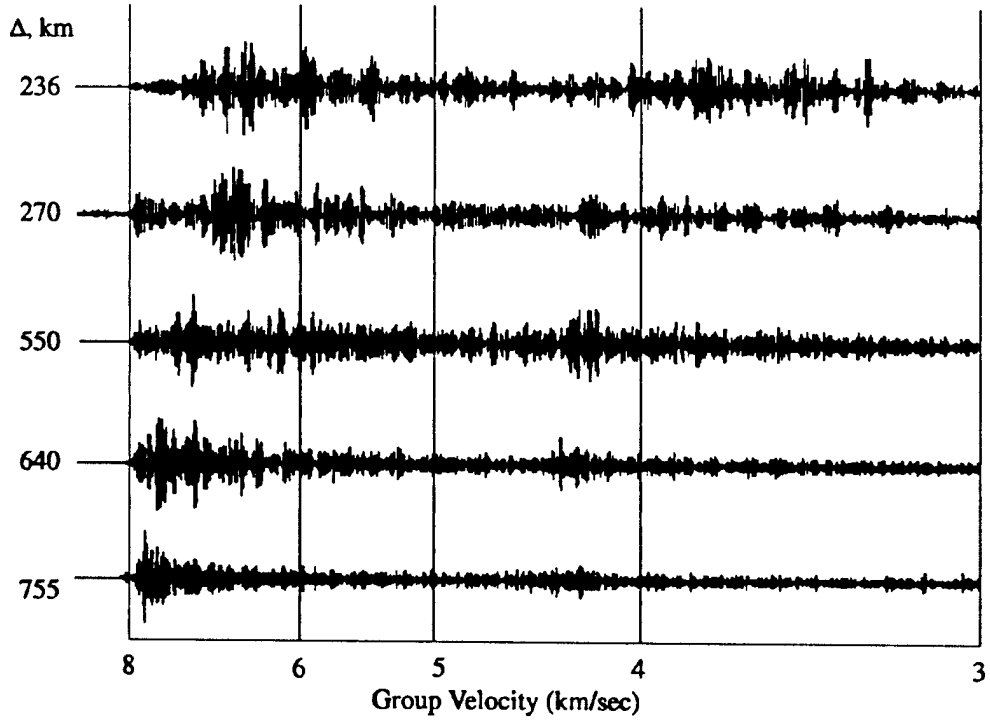

Figure 4-3. Bandpass filtered (6-8 Hz) vertical component regional signals for the selected Soviet PNE events of Figure 4-2.

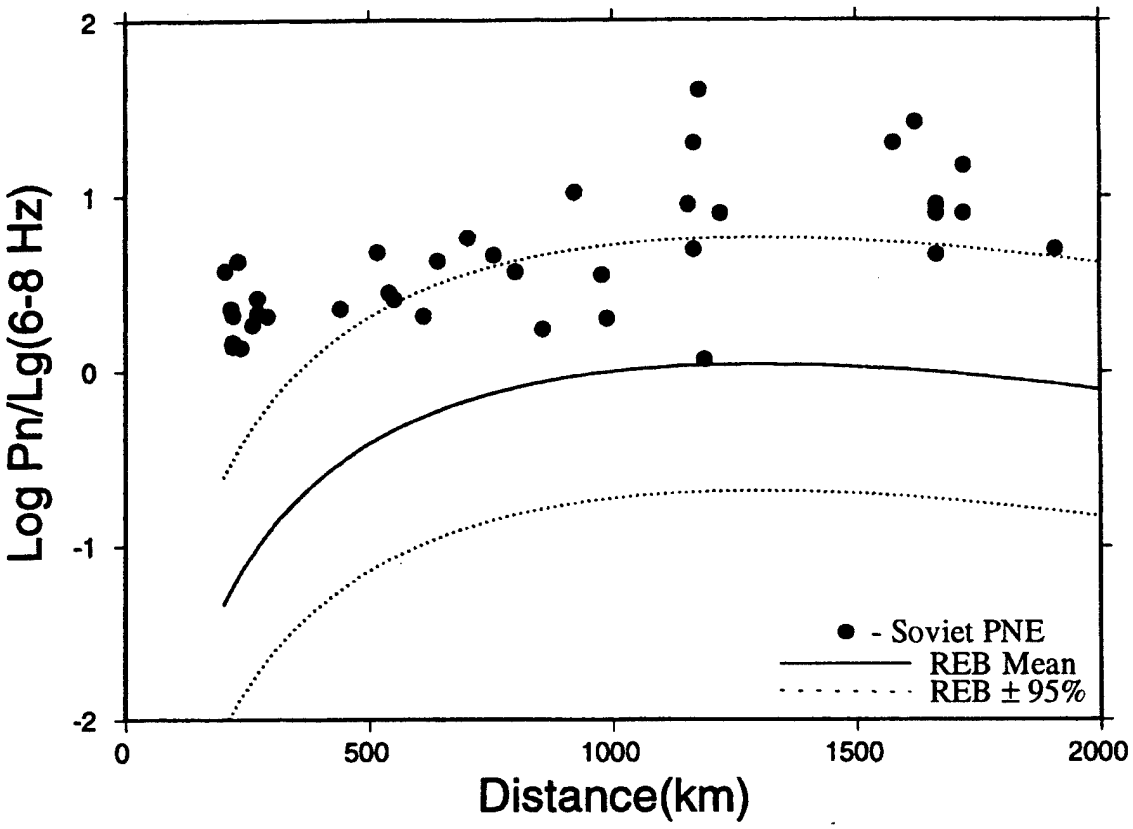

Figure 4-4. Comparison of 6-8 Hz Pn/Lg discriminant ratio values determined from broadband regional recordings of the selected Soviet PNE events with the corresponding mean and 2σ bounds on the REB earthquake population analyzed by Fisk et al (1999).

REB earthquake population analyzed by Fisk et al (1999). It can be seen from this figure that, although the means of the two populations are well separated, the two event distributions overlap significantly, with several of the PNE spectral discriminant values approaching the mean of the REB earthquake population. In fact, several of the PNE events which are problematical with respect to this prototype PIDC discriminant are among the group of explosions which caused problems in the lower frequency Borovoye discrimination analysis summarized in the previous section. Thus, it seems clear that propagation path effects are

responsible for at least some of these anomalous explosion values and Fisk et al (2000) are currently exploring various statistical techniques which might be used to account for such propagation path variability. In any case, these results indicate that the high frequency, prototype PIDC P_n/L_g spectral ratio discriminant will also have to be carefully calibrated for applications in previously untested areas.

SECTION 5

COMPARISON OF THE SEISMIC SOURCE CHARACTERISTICS OF NEARBY DEGELEN MOUNTAIN NUCLEAR AND CHEMICAL EXPLOSIONS

Prior to the initiation of nuclear testing at the Degelen Mountain area of the Semipalatinsk test site in 1961, a tamped chemical explosion (CE) was detonated in one of the tunnels to obtain ground motion calibration data. Approximately 4 months later, a companion nuclear explosion (NE) with a yield of 1.1 KT was detonated in an adjacent tunnel at nearly the same depth. A sketch illustrating the relative locations of these two explosions is shown in Figure 5-1 where it can be seen that they were separated by less than 1 km. The CE test was conducted on June 5, 1961 and consisted of 150 tons of fully tamped ammonium nitrate detonated in a rectangular chamber. Broadband seismic data were recorded from both events at the same stations located at distances of 39 and 84 km from the Degelen site, and these data provide another opportunity to compare the seismic source characteristics of these two types of tamped underground explosions.

The vertical component data recorded from the two explosions at the 39 and 84 km stations are compared in Figures 5-2 and 5-3, respectively, where it can be seen that the waveforms are fairly similar for the two source types, although the initial P waves from the NE event are more impulsive and simpler than those from the CE event, as might be expected. It can also be seen from these figures that the moveouts of the Rayleigh wave arrivals with respect to the corresponding initial P arrivals are greater for the NE event than for the CE event, which turns out to be consistent with the 1 km separation of the two explosions shown in Figure 5-1. More surprising is the fact that, once this relative group delay is accounted for, it

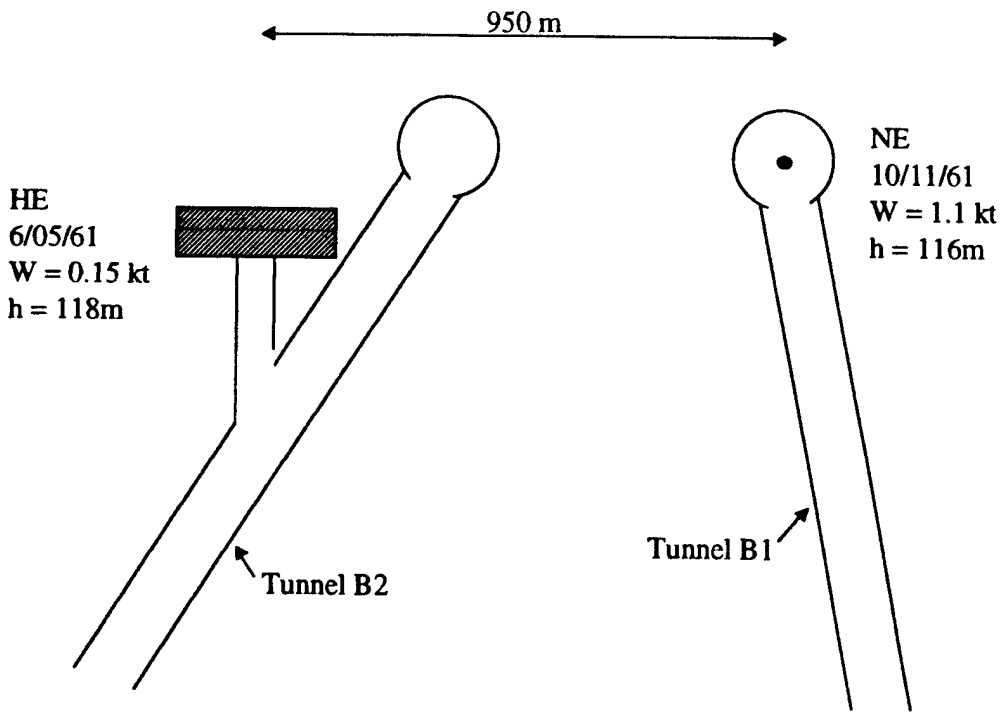

Figure 5-1. Schematic diagram showing the source configurations for the nearby 150 ton CE and 1.1 kt NE events detonated at Degelen Mountain in 1961.

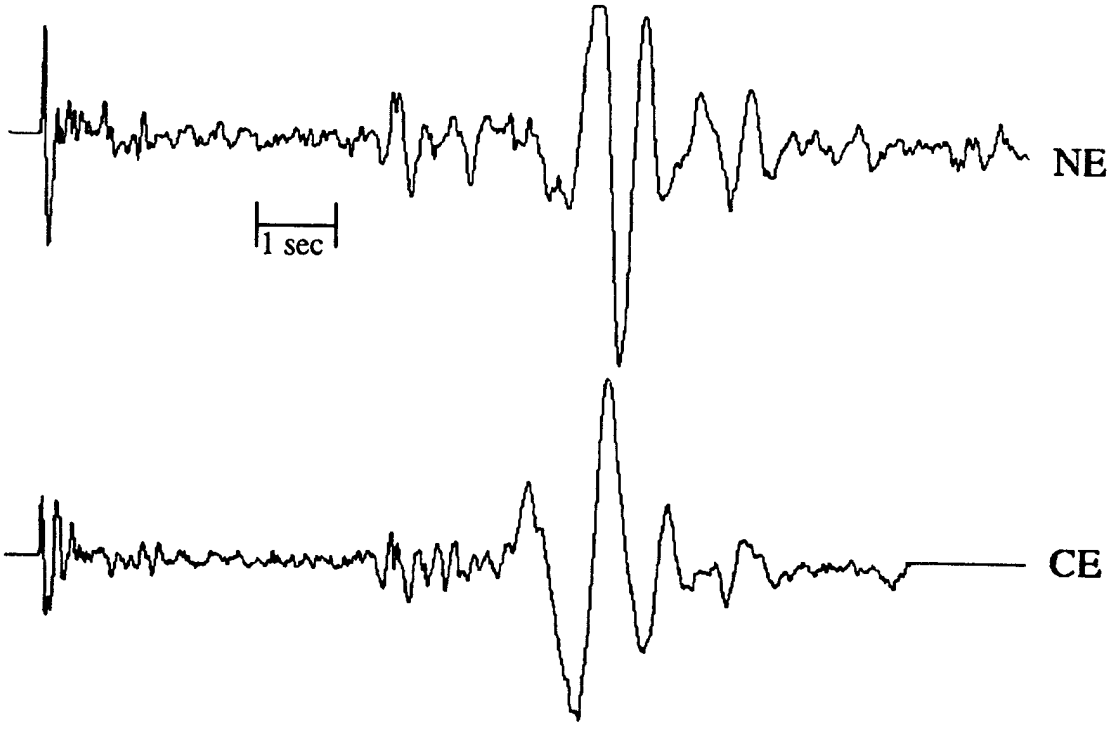

Figure 5-2. Comparison of vertical component recordings of the Degelen Mountain CE and NE events observed at a near-regional station at a range of 39 km.

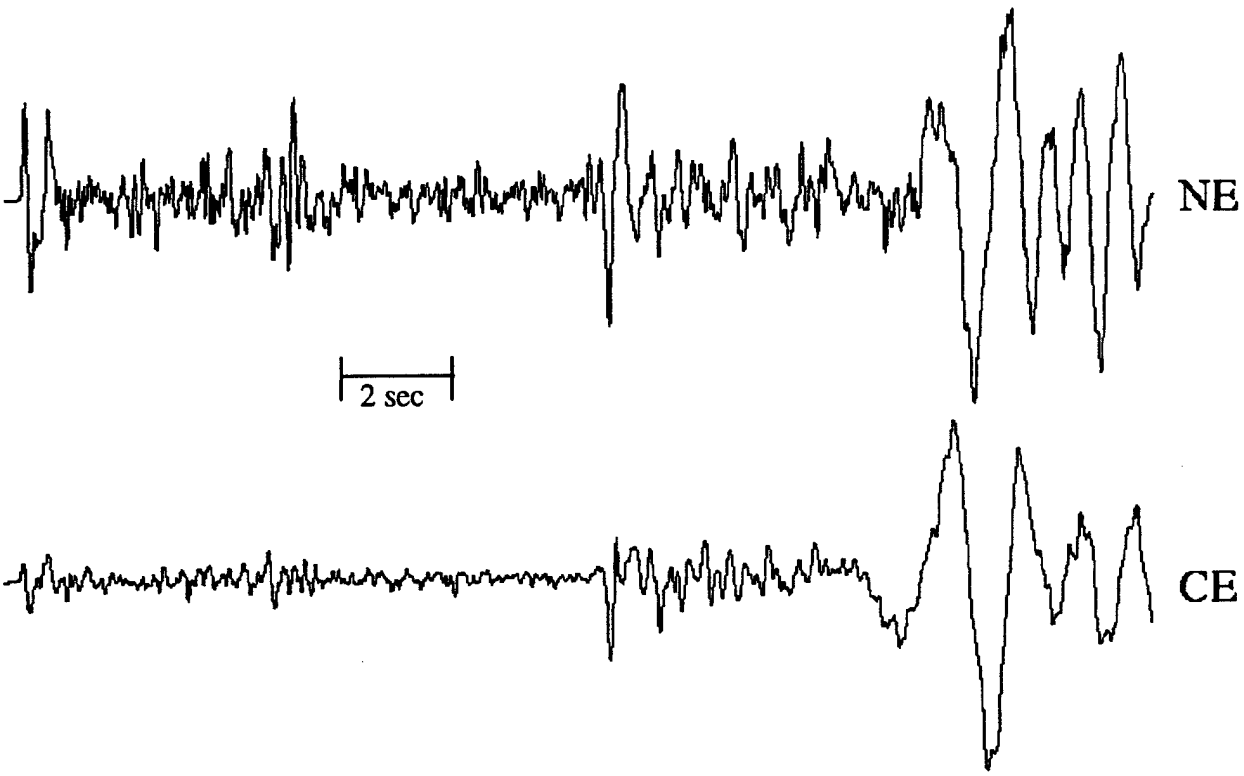

Figure 5-3. Comparison of vertical component recordings of the Degelen Mountain CE and NE events observed at a near-regional station at a range of 84 km.

appears that the Rayleigh waves from the two sources are 180 degrees out of phase, with that from the CE event appearing to be phase reversed with respect to that expected from a nominal explosion source. This observation is illustrated in Figure 5-4 where the time shifted and phase reversed Rayleigh waves from the CE event are shown overlain on the corresponding observed Rayleigh waves from the NE event. This observation may be an indication that significant tectonic strain energy release was triggered by the initial CE event and was therefore unavailable for release by the subsequent, nearby NE event, resulting in the observed relative Rayleigh wave phase reversal.

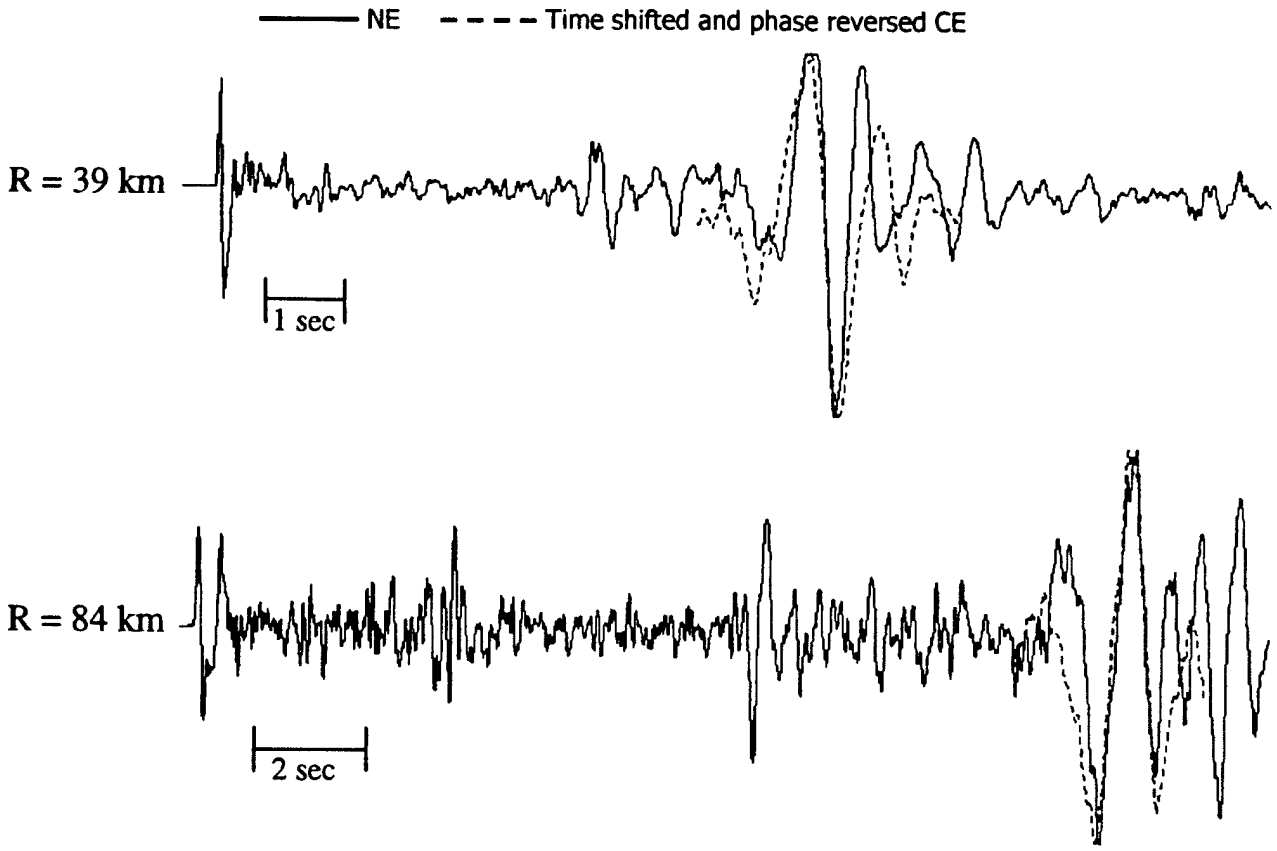

Figure 5-4. Comparison of vertical component NE recordings at 39 and 84 km with the corresponding CE Rayleigh wave recordings which have been phase reversed and time shifted to account for the propagation delay associated with the horizontal separation of the two sources.

The average NE/CE spectral ratios determined from the P and S wave time windows, as well as from the total vertical component recordings at the 39 and 84 km stations are compared in Figure 5-5 where it can be seen that they are all roughly independent of frequency over the range from 1 to 20 Hz, with average values ranging from about 7 to 10, which is roughly consistent with the direct ratio of the two yields (i.e. 7.3). Thus, in this case, it does not appear that the seismic coupling efficiency of the CE event was greater than that of the NE event by the often quoted factor of two. Moreover, it is surprising that the spectral ratios appear

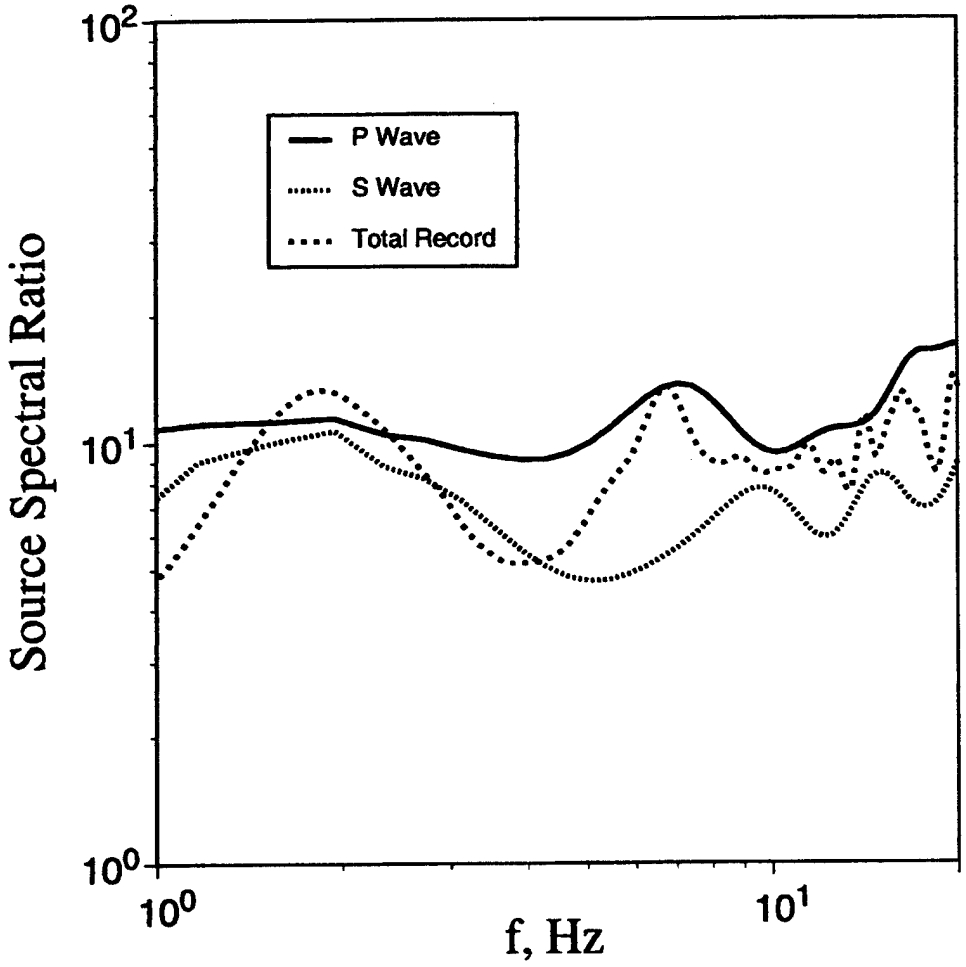

Figure 5-5. Average Degelen NE/CE source spectral ratios determined from data recorded at the 39 km and 84 km stations.

to be independent of frequency over the entire 1-20 Hz range, given the order of magnitude difference in the yields of the two explosions. Thus, for example, the approximate Mueller/Murphy explosion source model, which has been shown to be applicable to tamped Degelen Mountain NE events (Murphy, 1996), predicts source corner frequencies of about 5 and 10 Hz, respectively, for 1.1 KT and 150 ton explosions in Degelen granite. This prediction is illustrated in Figure 5-6 (left)

where the predicted seismic source functions corresponding to these two yields are compared. It follows that, as is illustrated in the right hand panel of this figure, according to conventional source theory the source spectral ratio of two such explosions would be expected to decrease significantly between about 5 and 10 Hz. However, no such decrease is evident in the observed source spectral ratios shown in Figure 5-5.

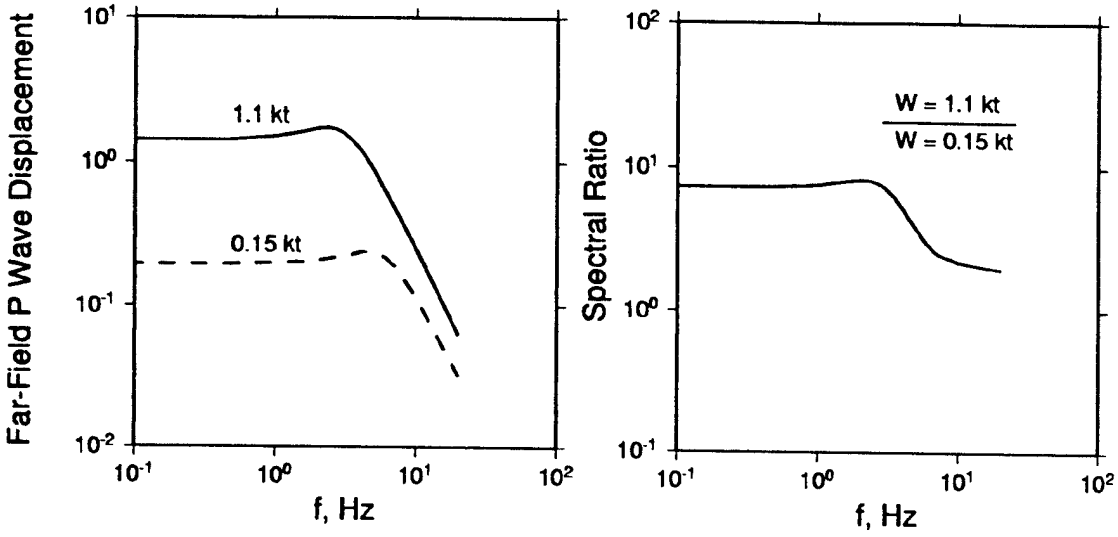

Figure 5-6. Comparison of far-field P wave displacement spectra (left) and associated source spectral ratio (right) corresponding to Mueller/Murphy granite source functions for 1.1 and 0.15 KT nuclear explosions in granite.

The simplest possible explanation for these discrepancies in the level and shape of this observed NE/CE source spectral ratio would be if the explosion efficiency of the CE test was somehow anomalous. However, no anomalous near-field observations were reported following this test, and this same explosive was used in a series of Soviet cavity decoupling tests conducted in Kirghizia in 1960 and

analyses of seismic data recorded from these tests indicated an explosive efficiency comparable to that of TNT (Murphy et al, 1997). An alternate possibility is that the tectonic release inferred from the observed Rayleigh wave phase reversal discussed previously may have affected both the amplitude level and frequency content of the CE seismic source. Supplemental free-field data would have to be recovered and analyzed to conclusively test this hypothesis.

SECTION 6

AN ANALYSIS OF EXPLOSION AFTERSHOCKS ASSOCIATED WITH SELECTED SOVIET PNE TESTS

6.1 BACKGROUND.

An underground nuclear detonation generates a primary seismic signal at the time of detonation and is the cause of many secondary seismic signals. Within milliseconds after the detonation of a contained nuclear explosion, a large spherical cavity is formed. This cavity is filled with a gas at high temperature and pressure that applies a force to the cavity wall. This force, together with the mechanical strength of the spherical dome, supports the weight of the material above the cavity. In time, the force applied by the gas decreases and if the mechanical strength of the dome is sufficient to support the material above the cavity, a free standing cavity will be formed. If the mechanical strength of the dome is insufficient, then at some point in time a cavity collapse will occur. As material falls into the cavity, a chimney of disturbed material is created as the original cavity void propagates toward the surface of the earth.

Experience has shown that collapse and associated chimney formation is a complex phenomenon and in many cases may be a multistage process. The initial collapse process may terminate at some point resulting in either a stable or quasi-stable void above the detonation point. For the quasi-stable case, the collapse will continue at some later time. Under certain conditions chimney growth may continue to the surface of the earth resulting in the formation of a surface subsidence crater. If a surface crater does not eventually form, either a partial collapse will occur resulting in a stable void above the original detonation point, or the volume associated with the original cavity void will be essentially distributed

in the chimney volume by a phenomena called bulking (density change), with chimney growth terminating below the earth's surface. In all cases, the process continues until one of the stable configurations defined above occurs.

In those cases involving cavity collapse and chimney growth, a portion of the kinetic energy of the falling material will be converted to seismic energy that is readily detectable with seismic instruments. In addition to the seismic signals associated with cavity collapse, other secondary signals, which are tectonic in origin, have been observed following some underground nuclear explosions. These signals, similar to naturally occurring earthquakes, are the result of a major disturbance in the natural stress patterns within the earth caused by the nuclear explosion. Both of these mechanisms have the potential for producing seismic data which may have applicability to onsite inspections under the CTBT. That is, given the existing uncertainties in IDC seismic locations, it will generally be necessary to initially employ a number of monitoring technologies in an attempt to zero in on the event location for onsite inspection purposes, and one of the primary techniques proposed for this purpose is the seismic detection of explosion induced aftershocks by temporary regional stations deployed for that purpose (Zucca et al., 1996). In order for this approach to be useful and reliable, it is necessary to have quantitative understanding of the dependence of aftershock activity on the explosion source characteristics. Most of the current state of knowledge regarding such explosion aftershocks is based on experience with explosions conducted at nominal containment depths at a few U.S. and Soviet nuclear weapons test sites. Thus, it is not clear how representative this experience is for the monitoring of small, deeply buried explosions in the variety of tectonic and geologic environments which must be considered in global monitoring of the CTBT. Aftershock monitoring data recorded from the more diverse Soviet PNE tests can

help to supplement these test site data to provide a more extensive experience base for use in defining onsite inspection strategy.

6.2 OVERVIEW OF NTS EXPERIENCE.

The cavity collapse process following underground nuclear explosions at NTS has been extensively investigated over the years, as evidenced by the fact that Springer and Kinnaman (1971, 1975) list collapse information for some 328 NTS explosions in their published seismic source summary for U.S. underground nuclear tests. Lynch (1978) analyzed this information, as well as a variety of other data available from NTS tests and reached the following general conclusions:

(1) Of the 464 explosions for which data were available in 1978, approximately 60% collapsed to the surface. However, no explosions with scaled depths $h/w^{1/3} >$ 250 $m/kt^{1/3}$ were observed to collapse to the surface.

(2) The observed times of collapse (either surface or subsurface) ranged from 1.7 minutes to over 6 years, with the following probabilities of occurrence:

65% in less than 1 hour
94% in less than 10 hours
96% in less than 1 day
98% in less than 1 year
2% 1-6 years

(3) In the absence of triggered tectonic activity, explosion aftershocks terminate with the end of the collapse signal. Thus, for environments analogous to NTS, it appears that fewer than 5% of the explosions would be expected to produce

aftershocks associated with cavity collapse which might be detected by an onsite inspection.

(4) There is at least one documented case at NTS for which a high sensitivity station at a distance of 6 km recorded **no** secondary signals, which suggests that a stable cavity may have been produced by this explosion.

Thus, a wide range of explosion aftershock activity has been observed at NTS and it is of interest to determine how typical this experience may be relative to what might be expected in the wide range of potential source environments which must be considered in global monitoring of the CTBT.

6.3 AFTERSHOCK MONITORING OF SELECTED SOVIET PNE TESTS.

As has been noted previously, Soviet PNE tests provide a unique basis for investigating verification capability with respect to the small, deeply buried explosions which are of greatest concern in CTBT monitoring. For this reason, a sample of 13 such explosions for which aftershock monitoring was carried out using data recorded from near-field stations has been selected for analysis. The map locations of these explosions these explosions are shown in Figure 6-1 where it can be seen that they are broadly distributed across the territories of the former Soviet Union. The location symbols on this figure distinguish between those PNE events for which aftershocks were observed and those for which no aftershocks were detected. Note that, in contrast to NTS experience, there are a significant number of Soviet PNE events for which no aftershock activity was detected. The source parameters of these 13 PNE events are listed in Table 6-1 where it can be seen that the explosions for which no aftershocks were observed encompass a wide variety of source media, yields and depths of burial, although most are

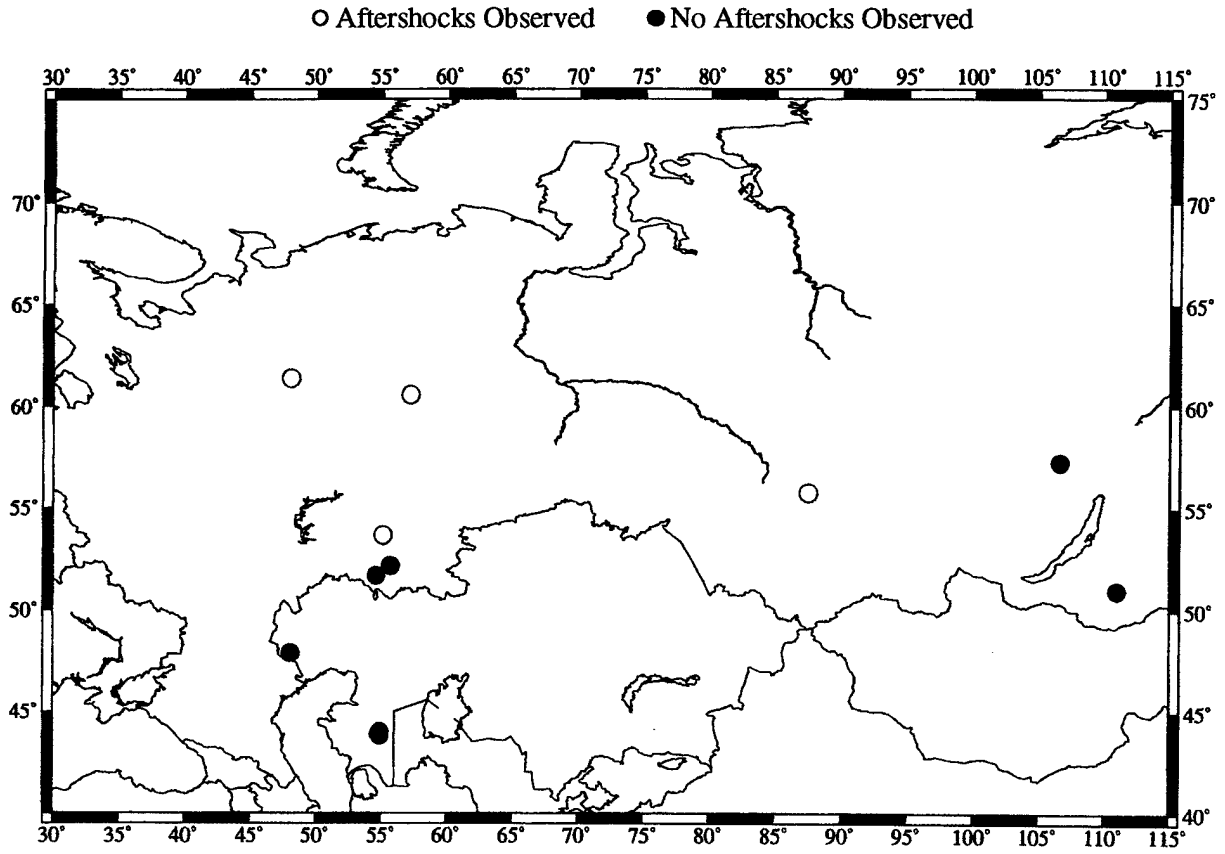

Figure 6-1. Map locations of Soviet PNE events for which onsite monitoring for aftershock activity was carried out.

significantly overburied relative to the nominal nuclear test site scaled depth of burial criterion. However, the four PNE events of Table 6-1 for which aftershocks were observed were also low yield, overburied explosions, so these can not be the only factors controlling the occurrence of aftershocks. For each of the four PNE events for which aftershocks were observed, the dependence of aftershock frequency of occurrence and magnitude on elapsed time after the explosion have been investigated in detail, and the results of these analyses are summarized in the following paragraphs.

Table 6-1. Source parameters of Soviet PNE events analyzed for explosion-induced aftershocks.

Aftershocks Observed

DATE	NAME	LAT, N	LON, E	YIELD, KT	h, m	MEDIUM
7/08/74	Kama-1	53.7	55.1	10	2123	limestone
9/17/84	Quartz-4	55.8	87.5	10	557	granite
4/19/87	Helium-3	60.6	57.2	3.2	2015	limestone
9/06/88	Ruby-1	61.4	48.1	7.5	793	anhydrite

No Observed Aftershocks

DATE	NAME	LAT, N	LON, E	YIELD, KT	h, m	MEDIUM
12/06/69	Mangyshlak-1	43.9	54.8	31	407	chalk
6/25/70	Magistral	52.2	55.7	2.3	702	salt
12/12/70	Mangyshlak-2	43.8	54.9	85	497	chalk
12/23/70	Mangyshlak-3	44.0	54.9	75	740	clay
12/22/71	Azgir 3-1	47.9	48.1	64	986	salt
4/11/72	Crater	37.3	62.1	14	1720	limestone
9/30/73	Sapphire-2	51.7	54.6	6.6	1145	salt
8/10/77	Meterorite-5	51.0	111.0	8.5	494	granite
9/10/77	Meterorite-4	44.0	54.9	75	740	clay

The Helium-3 PNE experiment consisted of two tests detonated 5 minutes apart at depths of about 2000m in limestone. Each explosion had a yield of 3.2 KT and the horizontal separation between the two was 1875m. Aftershock monitoring was conducted for a period of 11 hours after the explosions at a sensitive station located at a range of about 2 km from the two explosions. A total of 78 aftershocks were recorded from the two explosions, all of which occurred during the first 7.5 hours after the explosions. No further aftershocks were detected during the final 3.5 hours of monitoring, suggesting that the subsurface collapse processes terminated at 7.5 hours after detonation. Figure 6-2 shows a comparison of vertical and horizontal component recordings of one of the Helium-3 nuclear explosions with

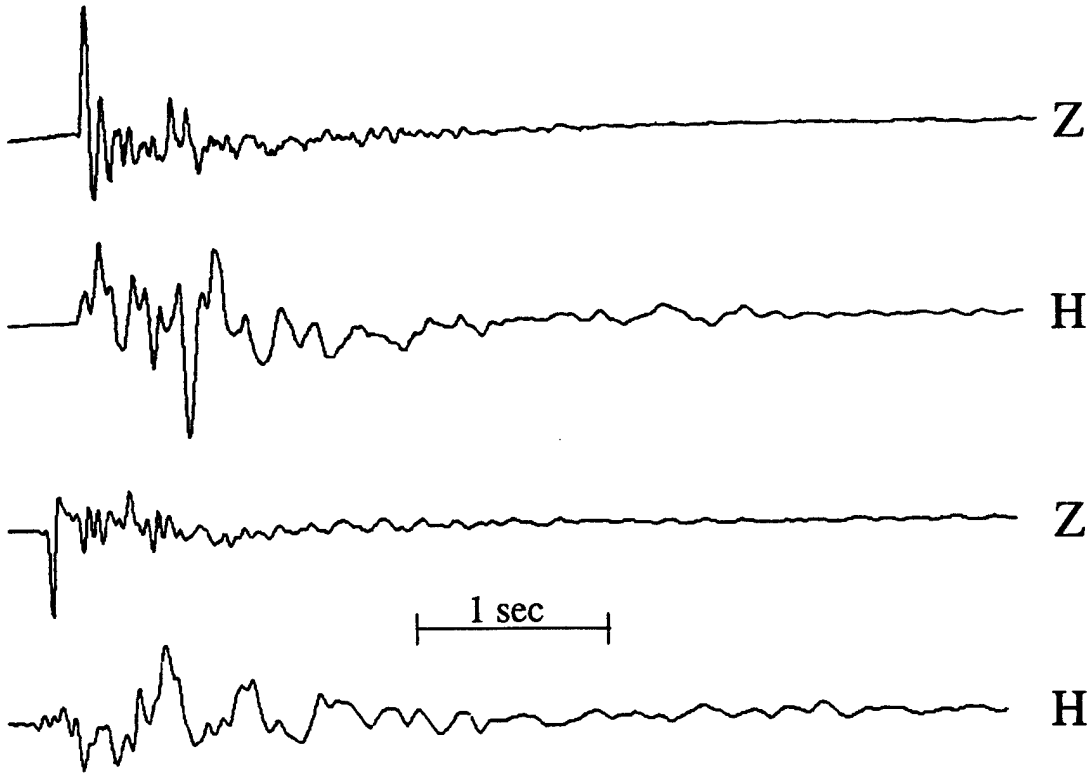

Figure 6-2. Comparison of vertical (Z) and horizontal (H) component recordings of one of the Helium-3 nuclear explosions (top) with those recorded at the same station from an explosion aftershock (bottom).

those recorded at the same station from one of the explosion aftershocks. It can be seen that the waveforms for the two source types are surprisingly similar with respect to duration and dominant frequency content, although the first motion for the aftershock is dilitational, which is typical of most aftershocks associated with the collapse process.

The relative peak displacements recorded from the Helium-3 aftershocks are plotted as a function of time after the second explosion in Figure 6-3, where it should be noted that the largest of these is smaller by a factor of 1000 than the corresponding peak displacements recorded from the PNE explosions. It can be

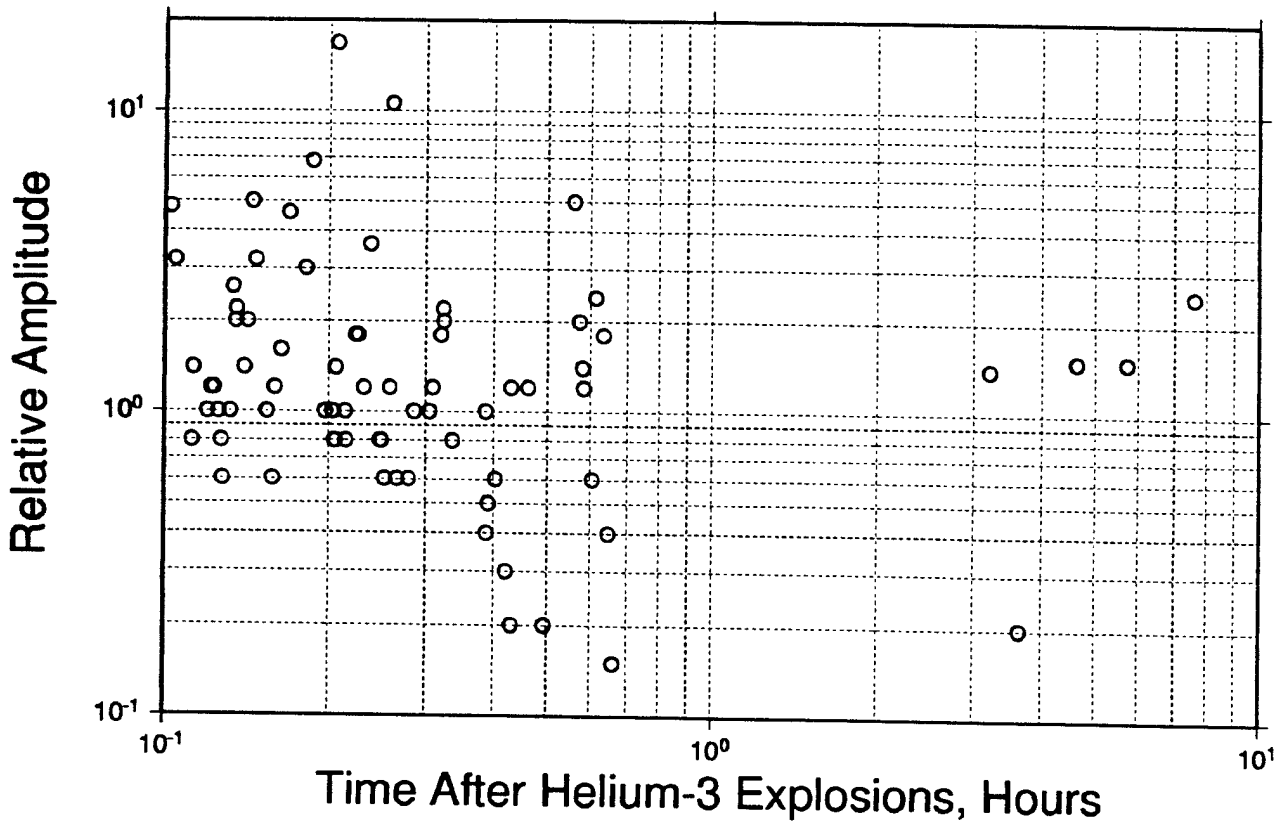

Figure 6-3. Peak displacements of the aftershocks of the Helium-3 explosions, plotted as a function of time after the second explosion.

seen from this plot that the aftershock activity decreased markedly about 40 minutes after the explosion, with only 5 occurring between 1 hour and the 7.5 hour termination of activity. Moreover, the peak displacements recorded from these last 5 events were all smaller than those recorded from the earlier, largest aftershocks by an order of magnitude or more. Thus, most significant triggered seismic activity ended after about 40 minutes.

Corresponding results for the other 3 Soviet PNE events which produced aftershocks may be briefly summarized as follows:

Kama-1 - Aftershock monitoring was conducted for 3 days following the explosion at a station located at a distance of about 10 km from the explosion. A total of 43 aftershocks were detected in the first 67 hours following the explosion, with the largest events occurring 40-47 minutes after the explosion and the rate of occurrence decreasing with time. No additional aftershocks were detected during the final 5 hours of monitoring.

Quartz 4 - Aftershock monitoring was conducted for 8 hours and 20 minutes following the explosion at a station located at a distance of about 1.7 km from the explosion. A total of 474 aftershocks were detected in the 7 hour and 12 minute period following the explosion, with the rate of occurrence decreasing to about 5/hour after the second hour. Aftershock activity was terminated by a large event (final cavity collapse?) at 7 hours and 12 minutes after the explosion. No additional aftershocks were detected during the final hour of monitoring.

Ruby-1 - Aftershock monitoring was conducted for 24 hours following the explosion at a station located at a distance of about 2 km from the explosion. A total of about 100 aftershocks were detected, but only 6 occurred more than 4 hours after the explosion. The last aftershock occurred 19 hours and 43 minutes after the explosion and no additional events were detected during the final 4 hours and 17 minutes of monitoring.

In summary, for that minority of Soviet PNE events examined with did produce aftershocks, the observations are fairly consistent with NTS experience in that aftershock activity effectively ends with what appears to be final, subsurface cavity collapse, which typically occurs within no more than a few days after the explosion.

SECTION 7
CONCLUSIONS

(1) A seismic source summary for Soviet PNE events has now been published (Sultanov et al, 1999) which lists the best currently available source parameters for 122 PNE experiments conducted between 1965 and 1988. These explosions represent a unique ground truth data source for use in regional calibration studies of areas encompassed by the territories of the former Soviet Union.

(2) Broadband regional seismic data recorded from a number of these PNE events and nearby earthquakes at the Borovoye station and other temporary stations have been systematically analyzed to quantify regional discrimination capability with respect to such events. The results of these analyses have indicated that, while the conventional high frequency S/P discriminants generally separate these explosion and earthquake populations, there is evidence that such discriminants will have to be carefully calibrated to account for regional propagation effects before they can be applied with high confidence in previously untested regions.

(3) A comparison of near-regional seismic signals recorded from nearby CE and NE events at Degelen Mountain has been completed and evidence has been found which indicates that tectonic release may also affect the seismic source characteristics of CE events, further complicating the seismic discrimination of these two types of tamped underground explosions.

(4) The results of near-field aftershock monitoring of a number of Soviet PNE events have been reviewed and it has been found that a surprisingly large number either produced no detectable aftershocks or produced brief aftershock sequences which ceased within 20 hours after the explosion. Such experience will have to be considered in evaluations of the reliability of aftershock monitoring to identify clandestine underground nuclear test locations during possible onsite inspections under the CTBT.

SECTION 8

REFERENCES

Adushkin, V. V, D. D. Sultanov, I. O. Kitov, and O. P. Kuznetsov (1992), "Overview of the experimental data and theoretical simulations of underground nuclear explosions decoupled by large air filled cavities," *Rep. Russian Acad. Sci., 327*, no. 1. (UNCLASSIFIED)

Fisk, M., S. Bottone, H. Gray and G. McCartor (1999), "Event Characterization Using Regional Seismic Data", Proceedings of the 21st Seismic Research Symposium: Technologies for Monitoring the Comprehensive Nuclear-Test-Ban Treaty, LA-UR-99-4700. (UNCLASSIFIED)

Fisk, M., S. Bottone and G. McCartor (2000), "Regional Seismic Event Characterization Using a Bayesian Kriging Approach", Proceedings of the 22nd Seismic Research Symposium, LA-UR-00-4700. (UNCLASSIFIED)

Kim, W-Y and G. Ekström (1996), "Instrument Responses of Digital Seismographs at Borovoye, Kazakhstan, by Inversion of Transient Calibration Pulses," *Bull. Seism. Soc. Am., 86*, 191. (UNCLASSIFIED)

Lynch, R. (1978), "A Preliminary Analysis of Seismic Phenomena Associated With the Collapse of Explosion Generated Cavities", CSC-TR-78-002. (UNCLASSIFIED)

Murphy, J. R. and T. J. Bennett (1982), "A Discrimination Analysis of Short-Period Regional Seismic Data Recorded at Tonto Forest Observatory," *Bull. Seism. Soc. Am., 72*, pp. 1351-1366. (UNCLASSIFIED)

Murphy, J. R., B. W. Barker and A. O'Donnell (1989), "Network-Averaged Teleseismic P-Wave Spectra For Underground Explosions. Part I. Definitions and Examples," *Bull. Seism. Soc. Am., 79*, 141-155. (UNCLASSIFIED)

Murphy, J. R., D. D. Sultanov, B. W. Barker, I. O. Kitov and M. E. Marshall (1996), "Application of Soviet PNE Data to the Assessment of the Transportability of Regional Discriminants," PL-TR-96-2290, ADA323142. (UNCLASSIFIED)

Murphy, J. R. (1996), "Types of Seismic Events and Their Source Descriptions," in *Monitoring a Comprehensive Test Ban Treaty, Proceedings of the NATO Advanced Study Institute*, Kluwer Academic Publishers, pp.225-245. (UNCLASSIFIED)

Murphy, J. R., I. O. Kitov, N. Rimer, D. D. Sultanov, B. W. Barker, J. L. Stevens, V. V. Adushkin and K. H. Lie (1996), "Further Studies of the Seismic Characteristics of Russian Explosions in Cavities: Implications For Cavity Decoupling of Underground Nuclear Explosions," PL-TR-96-2017, ADA305955. (UNCLASSIFIED)

Murphy, J. R., D. D. Sultanov, B. W. Barker, I. O. Kitov and M. E. Marshall (1997), "Further Analyses of Regional Seismic Data Recorded From the Soviet PNE Program: Implications With Respect to CTBT Monitoring", PL-TR-97-2141. (UNCLASSIFIED)

Murphy, J. R., I. O. Kitov, N. Rimer, V. V. Adushkin and B. W. Barker (1997), "Seismic Characteristics of Cavity Decoupled Explosions in Limestone: An Analysis of Soviet High Explosive Test Data," *Journal of Geophysical Research, 102*, B12, pp. 27, 393-27, 405. (UNCLASSIFIED)

Russian Federation Ministries of Atomic Energy and Defense (1996). "USSR nuclear weapon tests and peaceful nuclear explosions, 1949 through 1990," Russian Federation Nuclear Center, VNIIEF, ISBN 5-85165-062-1. (UNCLASSIFIED)

Springer, D. L. and R. L. Kinnaman (1971). "Seismic source summary for U.S. underground nuclear explosions, 1961-1970," *Bull. Seism. Soc. Am. 61*, 1073-1098. (UNCLASSIFIED)

Springer, D. L. and R. L. Kinnaman (1975). "Seismic source summary for U.S. underground nuclear explosions, 1971-1973," *Bull. Seism. Soc. Am. 65*, 343-349. (UNCLASSIFIED)

Sultanov, D. D., E. N. Ferapontova, P. B. Kaazik, I. O. Kitov, O. P. Kuznetsov, Yu. K. Malyshev, N. I. Nedoshivin, V. M. Ovtchinnikov, Kh. D. Rubinshtein and O. P. Willemson (1993), "Investigation of Seismic Efficiency of Soviet Peaceful Nuclear Explosions Conducted in Various Geological Conditions," ARPA Report under Contract MDA903-91-C-0151, Institute for Dynamics of the Geospheres, Russian Academy of Sciences. (UNCLASSIFIED)

Sultanov, D. D., J. R. Murphy and Kh. D. Rubinstein (1999), "A Seismic Source Summary For Peaceful Nuclear Explosions," *Bull. Seism. Soc. Am., 89*, pp. 640-647. (UNCLASSIFIED)

Zucca, J. J., C. Carrigan, P. Goldstein, S. Jarpe, J. Sweeney, W. L. Pickles and B. Wright (1996), "Signatures of Testing: On-Site Inspection Technologies" in *Monitoring a Comprehensive Test Ban Treaty, Proceedings of the NATO Advanced Study Institute*, Kluwer Academic Publishers. (UNCLASSIFIED)

DISTRIBUTION LIST

DTRA-TR-01-16

DEPARTMENT OF DEFENSE

DIRECTOR
DEFENSE INTELLIGENCE AGENCY
BUILDING 6000, BOLLING AFB
WASHINGTON, DC 20340 5100
ATTN: DTIB

DIRECTOR
DEFENSE RESEARCH & ENGINEERING
WASHINGTON, DC 20301 3110
ATTN: DDR&E, ROOM 3E808

DEFENSE TECHNICAL INFORMATION CENTER
8725 JOHN J KINGMAN, RD SUITE 0944
FORT BELVOIR, VA 22060 6218
2 CYS ATTN: DTIC/OCA

OFFICE OF THE SECRETARY OF DEFENSE
NUCLEAR TREATY PROGRMS OFFICE
1515 WILSON BOULEVARD, SUITE 720
ARLINGTON, VA 22209
ATTN: DR. MANGINO

DEPARTMENT OF AIR FORCE

AIR FORCE RESEARCH LABORATORY
5 WRIGHT STREET
HANSCOM AFB, MA 01731 - 3004
ATTN: RESEARCH LIBRARY, TL

AIR FORCE TECHNICAL APPLICATIONS CENTER
1300 17TH STREET, SUITE 1450
ARLINGTON, VA 22209
ATTN: R. BLANDFORD

AIR FORCE TECHNICAL APPLICATIONS CTR/TT
1030 S. HIGHWAY AIA
PATRICK AFB, FL 32925 - 3002
ATTN: CA, STINFO
ATTN: TTR, D. CLAUTER
ATTN: DR. B. KEMERAIT
ATTN: DR. D. RUSSELL
ATTN: TTR, F. SCHULT
ATTN: TTR, G. ROTHE
ATTN: M. SIBOL
ATTN: TTR, V. HSU

DEPARTMENT OF ENERGY

UNIVERSITY OF CALIFORNIA
LAWRENCE LIVERMORE NATIONAL LAB
P.O. BOX 808
LIVERMORE, CA 94551 - 9900
ATTN: MS L-205, DR. D. HARRIS
ATTN: K. NAKANISHI
ATTN: MS L-103, W.J. HANNON, JR
ATTN: MS L -200, TECHNICAL STAFF
ATTN: MS L-208, TECHNICAL STAFF
ATTN: MS L-205, TECHNICAL STAFF

LOS ALAMOS NATIONAL LABORATORY
P.O. BOX 1663
LOS ALAMOS, NM 87545
ATTN: MS, C335, DR. S. R. TAYLOR
ATTN: MS D460, F. CHAVEZ
ATTN: MS F607, D. STEEDMAN
ATTN: MS C335, TECHNICAL STAFF
ATTN: MS D460, TECHNICAL STAFF
ATTN: MS F665, TECHNICAL STAFF

PACIFIC NORTHWEST NATIONAL LABORATORY
P.O. BOX 999
BATTELLE BOULEVARD
RICHLAND, WA 99352
ATTN: MD K5-12, D N HAGEDORN

SANDIA NATIONAL LABORATORIES
MAIL SERVICES
P.O. BOX 5800
ALBUQUERQUE, NM 87185 - 1363
ATTN: TECHNICAL STAFF, DEPT 9311
MS 0813
ATTN: TECHNICAL STAFF, DEPT 5732,
MS 0979
ATTN: TECHNICAL STAFF, DEPT 5736,
MS 0572
ATTN: TECHNICAL STAFF, DEPT 5704,
MS 0655

OTHER GOVERNMENT

DEPARTMENT OF STATE
OES/NEP, ROOM 782-8
2201 C STREET, NW
WASHINGTON, DC 20520
ATTN: M. DREILER, ROOM 4953
ATTN: R. MORROW, ROOM 5741

US GEOLOGICAL SURVEY
ADVANCED SYSTEMS CENTER
MS 562
RESTON, VA 20192
ATTN: DR. J. FILSON
ATTN: W. LEITH

DEPARTMENT OF DEFENSE CONTRACTORS

BATTELLE MEMORIAL INSTITUTE
MUNITIONS & ORDNANCE CTR
505 KINGS AVENUE
COLUMBUS, OH 43201 - 2693
ATTN: TACTEC

BBN CORPORATION
1300 N. 17TH STREET, SUITE 1200
ARLINGTON, VA 22209
ATTN: DR. D. NORRIS
ATTN: H. FARRELL
ATTN: J. PULLI

CENTER FOR MONITORING RESEARCH
1300 N. 17TH STREET, SUITE 1450
ARLINGTON, VA 22209
ATTN: DR. K. L. MCLAUGHLIN
ATTN: DR. R. WOODWARD
ATTN: DR. R. NORTH
ATTN: DR. V. ROYABOY
ATTN: DR. X. YANG
ATTN: LIBRARIAN

ENSCO, INC.
4849 N WICKHAM RD
MELBOURNE, FL 32940
ATTN: DR. D. TAYLOR

ENSCO, INC.
P.O. BOX 1346
SPRINGFIELD, VA 22151 - 0346
ATTN: D. BAUMGARDT
ATTN: Z. DER

GEOPHEX, LTD
WESTON GEOPHYSICAL
325 WEST MAIN STREET
NORTHBOROUGH, MA 01532
ATTN: DR. D. REITER
ATTN: MR. J. LEWKOWICZ

ITT INDUSTRIES
ITT SYTEMS CORPORATION
1680 TEXAS STREET SE
KIRTLAND AFB, NM 87117 - 5669
2 CYS ATTN: DTRIAC
ATTN: DARE

MAXWELL LABORATORIES, INC.
S-CUBED WASHINGTON RESEARCH OFFICE
11800 SUNRISE VALLEY DRIVE, SUITE 1212
RESTON, VA 22091
ATTN: DR. T. J. BENNETT
ATTN: J. MURPHY

MISSION RESEARCH CORPORATION
8560 CINDERBED ROAD, SUITE 700
NEWINGTON, VA 22122
ATTN: DR.M. FISK

MISSION RESEARCH CORPORATION
P.O. BOX 719
SANTA BARBARA, CA 93102 - 0719
ATTN: DR. S. BOTTONE

MULTIMAX, INC
1441 MCCORMICK DRIVE
LANDOVER, MD 20786
ATTN: DR. I. N. GUPTA
ATTN: DR. W. CHAN

SCIENCE APPLICATIONS INT'L CORPORATION
10260 CAMPUS POINT DRIVE
SAN DIEGO, CA 92121 - 1578
ATTN: DR. A. BAKER
ATTN: DR. G. KENT
ATTN: J. STEVENS
ATTN: T.C. BACHE, JR.
ATTN: T.J. SERENO, JR.

ST LOUIS UNIVERSITY
P.O. BOX 8148
PIERRE LACLEDE STATION
ST LOUIS, MO 63156 - 8148
ATTN: PROF B. J. MITCHELL
ATTN: PROF R. HERRMAN

TITAN CORPORATION (ATS)
1900 CAMPUS COMMONS DR.
SUITE 600
RESTON, VA 20191-1535
ATTN: DR C P KNOWLES

TITAN PULSE SCIENCE DIVISION
2700 MERCED ST
SAN LEANDRO, CA 94577- 0599
ATTN: B.W. BARKER
ATTN: J.R. MURPHY
ATTN: M.E. MARSHALL

TEXAS UNIVERSITY AT AUSTIN
P.O. BOX 7726
AUSTIN, TX 78712
ATTN: DEPT EARTH PLANET SCI

URS CORP CORPORATION
586 EL DORADO STREET
PASADENA, CA 91109 - 3245
ATTN: DR. B. B. WOODS
ATTN: DR. C. K. SAIKIA

FOREIGN
AUSTRALIAN GEOLOGICAL SURVEY
ORGANIZATION
CORNER OF JERRAGOMRRRA&
NINDMARSH DRIVE
CANBERRA, ACT 2609
AUSTRALIA
ATTN: D. JEPSON

GEOPHYSICAL INSTITUTE OF ISRAEL
POB 182
LOD, 71100 ISRAEL
ATTN: DR. Y. GITTERMAN
ATTN: DR. A. SHAPIRA

I.R.I.G.M. - B.P. 68
38402 ST MARTIN D'HERES
CEDEX, FRANCE
ATTN: DR. M. BOUCHON

MINISTRY OF DEFENSE
PROCURMENT EXECUTIVE
BLACKNESS, BRIMPTON
READING FG7-4RS ENGLAND
ATTN: DR. P. MARSHALL

NTNF/NORSAR
P.O. BOX 51
N-2007 KJELLER, NORWAY
ATTN: DR. F. RINGDAL
ATTN: T. KVAERNA

OBSERVATORIE DE GRENOBLE
I.R.I.G.M. - B.P. 53
38041 GRENOBLE, FRANCE
ATTN: DR. M. CAMPILLO

RESEARCH SCHOOL OF EARTH SCIENCES
INSTITUTE OF ADVANCED STUDIES
G.P.O. BOX 4
CANABERRA 2601, AUSTRALIA
ATTN: PROF B.L. N. KENNETT

RUHR UNIVERSITY/BOCHUM
INSTITUTE FOR GOEPHYSIK
P.O. BOX 102148
463 BOCHUM 1, GERMANY
ATTN: PROF. H.P. HARJES

UNIVERSITY OF BERGEN
INSTITUTE FOR SOLID EARTH PHYSICS
ALLEGATON 41
N-5007 BERGEN, NORWAY
ATTN: R.E. HUSEBYE

DIRECTORY OF OTHER (LIBARIES AND UNIVERSITIES)

ARIZONA UNVIERSITY OF
DEPARTMENT OF GEOSCIENCES/SASO
TUCSON, AZ 85721
ATTN: PROF. T.C. WALLACE

BOISE STATE UNIVERSITY
GEOSCIENCES DEPARTMENT
1910 UNIVERSITY DRIVE
BOISE, ID 83725
ATTN: J.E. ZOLLWEG

DISTRIBUTION LIST

DTRA-TR- 01 - 16

BOSTON COLLEGE
INSTITUTE FOR SPACE RESEARCH
140 COMMONWEALTH AVENUE
CHESTNUT HILL, MA 02167
ATTN: DR. D. HARKRIDER
ATTN: B. SULLIVAN

BROWN UNIVERSITY
DEPARTMENT OF GEOLOGICAL SCIENCES
75 WATERMAN STREET
PROVIDENCE, RI 02912 - 1846
ATTN: PROF. D. FORSYTH

CALIFORNIA INSTITUTE OF TECHNOLOGY
DIVISION OF GEOLOGY & PLANETARY SCIENCES
PASADENA, CA 91125
ATTN: PROF. D.V. HELMBERGER
ATTN: PROF. T. AHRENS

CALIFORNIA - BERKELEY, UNIVERSITY OF
DOE LIBRARY
BERKELEY, CA 94720 - 2599
ATTN: PROF. B. ROMANOWICZ
ATTN: PROF. L. JOHNSON

CALIFORNIA - DAVIS, UNIVERSITY OF
ONE SHIELDS AV
DAVIS, CA 95616
ATTN: R.H. SHUMWAY, DIV STATISTICS

CALIFORNIA - SAN DIEGO, UNIVERSITY OF
9500 GILMAN DR
LA JOLLA, CA 92093 - 0225
ATTN: DR. L. DEGROOT - HEDLIN
ATTN: DR. M. HEDLIN
ATTN: PROF. F. VERNON
ATTN: PROF. J. BERGER
ATTN: PROF. J. ORCUTT

CALIFORNIA - SANTA CRUZ, UNIVERSITY OF
INSTITUTE OF TECTONICS
1156 HIGH ST
SANTA CRUZ, CA 95064
ATTN: DR. R.S. WU
ATTN: PROF. T. LAY

COLORADO - BOULDER, UNIVERSITY OF
CAMPUS BOX 390
BOULDER, CO 80309
ATTN: DR R ENGDAHL
ATTN: M RITZWOLLER

COLUMBIA UNIVERSITY
LAMONT-DOHERTY EARTH OBSERVATORY
2960 BROADWAY ST.
PALISADES, NY 10964
ATTN: DR. L.R. SYKES
ATTN: DR. J. XIE
ATTN: DR. W. Y. KIM
ATTN: PROF. P.G. RICHARDS

CONNECTICUT, UNIVERSITY OF
DEPARTMENT OF GEOLOGY & GEOPHYISCS
354 MANSFIELD RD. UNIT 2045
STOOTS, CT 06269 - 2045
ATTN: PROF .V.F. CORMIER, U-45, RM 207

CORNELL UNIVERSITY
DEPARTMENT OF GEOLOGICAL SCIENCES
3126 SNEE HALL
ITHACA, NY 14853
ATTN: PROF. M. BARAZANGI

HARVARD UNIVERSITY
HOFFMAN LABORATORY
20 OXFORD STREET
CAMBRIDGE, MA 02138
ATTN: PROF. A. DZIEWONSKI
ATTN: PROF. G. EKSTROM

INDIANA UNIVERSITY
DEPARTMENT OF GEOLOGICAL SCIENCES
1005 10TH STREET
BLOOMINGTON, IN 47405
ATTN: PROF. G. PAVLIS

IRIS
1200 NEW YORK AVENUE, NW SUITE 800
WASHINGTON, DC 20005
ATTN: DR. D. SIMPSON
ATTN: DR. G .E. VAN DER VINK

MASSACHUSETTS INSTITUTE OF TECHNOLOGY
EARTH RESOURCES LABORATORY
42 CARLETON ST.
CAMBRIDGE, MA 02142
ATTN: DR. W. RODI
ATTN: PROF. M. N. TOKSOZ

MICHIGAN STATE UNIVERSITY LIBRARY
450 ADMINISTRATION BUILDING
EAST LANSING, MI 48824
ATTN: KAZUYA FUJITA

NEW MEXICO STATE UNIVERSITY
DEPARTMENT OF PHYSICS
PO BOX 30001
LAS CRUCES, NM 88003
ATTN: PROF. J. NI
ATTN: PROF T. HEARIN

NORTHWESTERN UNIVERSITY
DEPARTMENT OF GEOLOGICAL SCIENCES
1847 SHERIDAN RD
EVANSTON, IL 60208
ATTN: PROF. E. OKAL

PENNSYLVANIA STATE UNIVERSITY
GEOSCIENCES DEPARTMENT
403 DEIKE BUILDING
UNIVERSITY PARK, PA 16802
ATTN: PROF. C. A. LANGTSON
ATTN: PROF. S. ALEXANDER

SAN DIEGO STATE UNIVERSITY
DEPARTMENT OF GEOLOGICAL SCIENCES
5500 CAMPANILE DR.
SAN DIEGO, CA 92182
ATTN: PROF. S.M. DAY

SOUTHERN METHODIST UNIVERSITY
P.O. BOX 750395
DALLAS, TX 75275
ATTN: B. STUMP, DEPARTMENT OF GEOLOGICAL SCIENCES
ATTN: E. HERRIN, DEPARTMENT OF GEOLOGICAL SCIENCES
ATTN: G. MCCARTOR, DEPARTMENT OF PHYSICS
ATTN: H.L. GRAY, DEPARTMENT OF STATISTICS

UNIVERSITY OF HAWAII - MANOA
P.O. BOX 1599
KAILUA - KONA, HI 96745 - 1599
ATTN: DR. M. A. GARCES

UNIVERSITY OF IDAHO
DEPARTMENT OF GEOLOGY
MOSCOW, ID 83844
ATTN: PROF. K. SPRENKE

UNIVERSITY OF SOUTHERN CALIIFORNIA
520 SEAVER SCIENCE CENTER
UNIVERSITY PARK
LOS ANGELES, CA 90089 - 0483
ATTN: PROF. C.G. SAMMIS

WASHINGTON UNIVERSITY
ONE BROOKINGS DRIVE
SAINT LOUIS, MO 63130 - 4899
ATTN: DR. G. SMITH, DEPARTMENT EARTH PLANET SCI